Kingdom of Saudi Arabia
King Abdulaziz City For Science and Technology
General Directorate of Research Grants Programs

AR – 20 – 68

REVISED FINAL REPORT

IMPROVING THE LEVEL OF SEISMIC HAZARD PARAMETERS IN SAUDI ARABIA USING EARTHQUAKE LOCATION AND MAGNITUDE CALIBRATION

Dr. Abdullah M. Al-Amri, KSU (P-I)
Dr. Tariq A. Alkhalifah, KACST (CO-I)

KING SAUD UNIVERSITY

RABI' I 1425 H – MAY 2004 A.D

المملكه العربيه السعوديه
مدينة الملك عبدالعزيز للعلوم والتقنيه
الإداره العامه لبرامج المنح

المشروع البحثي ٢٠ - ٦٨

التقرير النهائي المنقح

تحسين معاملات مستوى الخطر الزلزالي في المملكه العربيه السعوديه بإستخدام موقع الزلزال ومعايرة قدره

د. عبدالله بن محمد العمري (الباحث الرئيس)
د. طارق بن علي الخليفه (الباحث المشارك)

جامعة الملك سعود
ربيع الاول ١٤٢٥هـ - مايو ٢٠٠٤م

ACKNOWLEDGMENTS

This is the final progress report of the research project **AR-20-68** . The authors would like to express their thanks and gratitude to King Abdulaziz City for Science and Technology for funding this project. This work would not have been possible without the generous assistance of **KACST** and **KSU**.

Dr. Arthur Rodgers, the project consultant, whose expert guidance and continuing advice made this work possible. His willingness to devote his time greatly facilitated the completion of the project We owe him a deep debt of gratitude and a great deal of thanks. Grateful acknowledgment is also extended to the anonymous referees for their helpful suggestions and criticism.

Finally and most importantly, we would like to extend our sincerest thanks to Engineers Moustafa Hameda from KACST and Ahmed R. Khalil from KSU for providing this project with the earthquake data and to Dr. Michael Pasyanos and Ms. Maggie Benoit who performed the surface wave group velocity measurements and tomography.

الخلاصه

يشتمل التقرير النهائي المنقح من المشروع البحثي التطبيقي أت-٢٠-٦٨ على نتائج التقارير الدورية الثلاثة السابقة بالاضافه إلى نتائج المرحلة النهائية من هذه الدراسة ومرئيات المحكمين على التقرير النهائي وذلك لغرض تحسين معاملات الخطر الزلزالي في مختلف مناطق المملكه من خلال تحديد موقع الزلزال ومعايرة قدره .

على الرغم من قلة النشاط الزلزالي في معظم مناطق المملكه وخاصة الدرع العربي والمسطح العربي إلا أن قربها من المناطق النشطه زلزالًيا في إيران وتركيا من ناحية الشمال الشرقي والبحر الأحمر والدرع العربي من جهة الغرب والجنوب الغربي وصدع البحر الميت التحولي شمالاً يتطلب دراسة مواقع الزلازل بدقة عاليه للإستفاده منها في تحديد مناطق الخطر الزلزالي المحتمل .

يشتمل التقرير النهائي المنقح على تحليل المعلومات الزلزاليه وأزمنة المسار ونمذجة الشكل الموجي للمعلومات الرقمية التي سجلتها الشبكه الوطنيه للزلازل التابعة لمدينة الملك عبدالعزيز للعلوم والتقنيه. وتقوم الشبكة حالًيا بتشغيل ٢٧ محطة رقميه واسعة المدى و ١١ محطه قصيرة المدى. وتتميز محطات هذه الشبكه بقدرتها العاليه على إلتقاط الإشارات الزلزاليه المحلية والاقليميه وهذا يعود إلى هدوء مواقع المحطات الحقليه.

تم في هذا المشروع دراسة خواص الضوضاء السيزميه في محطات الشبكه و مقارنة مواقع الزلازل الإقليميه التي سجلتها شبكة المدينه مع المواقع التي سجلتها الشبكات الدوليه. يعود سبب الإختلاف الكبير بين هذه المواقع إلى أن نموذج تحليل المواقع المستخدم حالًيا في المدينة Iasp91 غير مناسب.

وعلى ضوء ذلك قامت هذه الدراسه بتحليل دقيق لعدة زلازل إقليميه ودراسة تفجيرات البحر الميت وتم حساب الأخطاء في تحديد المواقع ومعايرة الاقدار الزلزاليه. كما تم إستنتاج ثلاثة نماذج للسرع الزلزاليه لشبه الجزيرة العربيه لكل من :

١. منطقة خليج العقبه والبحر الميت

٢. الدرع العربي

٣. المسطح العربي

هذه النماذج تم تطبيقها حاليا في شبكة المدينه والتي سوف تؤدي إلى تحسين مواقع الزلازل المحليه والإقليميه وتحديد أقدارها بدقة متناهيه.

ABSTRACT

This revised final report of the research project AR-20-68 culminates the study reported earlier in the three progress reports as well as reviewer's comments and suggestions on the final report. The objective of the proposed research is to improve assessment of seismic hazard parameters by improving earthquake location and magnitude estimates with the Saudi Arabian National Digital Seismic Network **(SANDSN).**

While for the most parts of Saudi Arabia, particularly, Arabian Shield and Arabian Platform a aseismic, the area is ringed with regional seismic sources in the tectonically active areas of Iran and Turkey to the northeast, the Red Sea Rift bordering the Shield to the southwest, and the Dead Sea Transform fault zone to the north.

This report describes research performed to analyze earthquake data, travel times and seismic waveform data from the **SANDSN**. **KACST** operates the 38 station **SANDSN**, consisting of 27 broadband and 11 short-period stations. The **SANDSN** has good signal detection capabilities because the sites are relatively quiet. Research was performed to characterize seismic background noise at various stations in the network.

Locations of regional earthquakes estimated by **KACST** were compared with locations from global bulletins. Large differences between **KACST** and global catalog locations are likely the result of inadequacies of the global average earth model **(iasp91)** used by the **KACST** system.

We present detailed analysis of some events and Dead Sea explosions where we found gross errors in estimated locations. Velocity models are presented that should improve estimated locations of regional events in three specific regions: 1. Gulf of Aqabah - Dead Sea region

2. Arabian Shield and 3. Arabian Platform.

Recently, these models were applied to the **SANDSN** to improve local and teleseismic event locations and to develop an accurate magnitude scale for Saudi Arabia.

TABLE OF CONTENTS

LIST OF TABLES

LIST OF FIGURES

1. INTRODUCTION

There has only been a modest amount of earthquake seismological work done in the Arabian Peninsula. Several countries either on or surrounding the Peninsula have seismograph stations, but most stations are equipped with short-period vertical seismometers. In any event, the networks are sparse and often are poorly situated with respect to seismically active areas. Broadband data required for analysis of teleseismic receiver functions are almost wholly lacking. Regional wave propagation from earthquakes and seismic wave attenuation have not been studied. Microseismicity is known to occur in many areas of the Peninsula, but the existing network of stations is inadequate for accurately defining spatial characteristics or determining focal mechanisms.

In January, 2002 , we set-up SUN Ultra 80 workstation at the KSU Seismic Studies Center for the project. We installed Generic Mapping Tool (GMT) mapping software and Seismic Analysis Code (SAC) as well as various system software tools. Books and manuals for the UNIX operating system were delivered. KSU and KACST personnel were trained on the operation of software tools.

One of the main objectives of this proposal is to estimate crustal and upper mantle structure to improve earthquake location and magnitude estimation. While there have been many studies of this topic using a wide variety of techniques, many questions about the structure of the Arabian Peninsula remain unanswered. A thorough understanding of the seismic structure and wave propagation characteristics of the region must be established before we can proceed to assess seismic hazard. Therefore, the objective of the proposed research is to improve assessment of seismic hazard parameters by improving earthquake location and magnitude estimates with the Saudi National Seismic Network (SANDSN).

The results obtained from this research are :

1. Refined travel time curves of regional seismic phases (Pn, Pg, Sn and Lg) and seismic velocity models to improve earthquake location accuracy;
2. Development of an accurate magnitude scale for Saudi Arabia and surrounding regions;
3. Estimates of earthquake moments, focal mechanisms and depths and refinements of velocity models from long-period waveform modeling;
4. Application of research results to improve location and magnitude estimates by SANDSN researchers; and
5. Advancement of basic knowledge of seismic and tectonic structure of the lithosphere.

2. SEISMOTECTONICS & SEISMIC STRUCTURES

The Arabian Peninsula forms a single tectonic plate, the Arabian Plate. It is surrounded on all sides by active plate boundaries as evidenced by earthquake locations. Figure 1 shows a map of the Arabian Peninsula along with major tectonic features and earthquake locations. Active tectonics of the region is dominated by the collision of the Arabian Plate with the Eurasian Plate along the Zagros and Bitlis Thrust systems, rifting and seafloor spreading in the Red Sea and Gulf of Aden. Strike-slip faulting occurs along the Gulf of Aqabah and Dead Sea Transform fault systems. The great number of earthquakes in the Gulf of Aqabah pose a significant seismic hazard to Saudi Arabia. Large earthquakes in the Zagros Mountains of southern Iran may lead to long-period ground motion in eastern Saudi Arabia.

The two large regions associated with the presence or absence of sedimentary cover define the large-scale geologic structure of the Arabian Peninsula. The Arabian Platform (eastern Arabia) is covered by sediments that thicken toward the Arabian Gulf. The Arabian Shield is has no appreciable sedimentary cover with many outcrops. Figure 2 shows the sediment thickness, estimated from compiled drill hole, gravity and seismic reflection data *(Seber et al.,* 1997*).* The Arabian Shield consists of at least five Precambrian terranes separated by suture zones (*Schmidt et al*., 1979). During the late Oligocene and early Miocene, the Arabian Shield was disrupted by the development of the Red Sea and Gulf of Aden rifts, and from the mid-Miocene to the present, the region experienced volcanism and uplift (*Bohannon et al.,* 1989). The uplift and volcanism are generally assumed to be the result of hot, buoyant material in the upper mantle that may have eroded the base of the lithosphere (*Camp and Roobol*, 1992). However details about the nature of the upper mantle, such as its thermal and compositional state, are not known. Volcanic activity (the Harrats) is observed on the Arabian Shield (Figure 1). This is likely to be

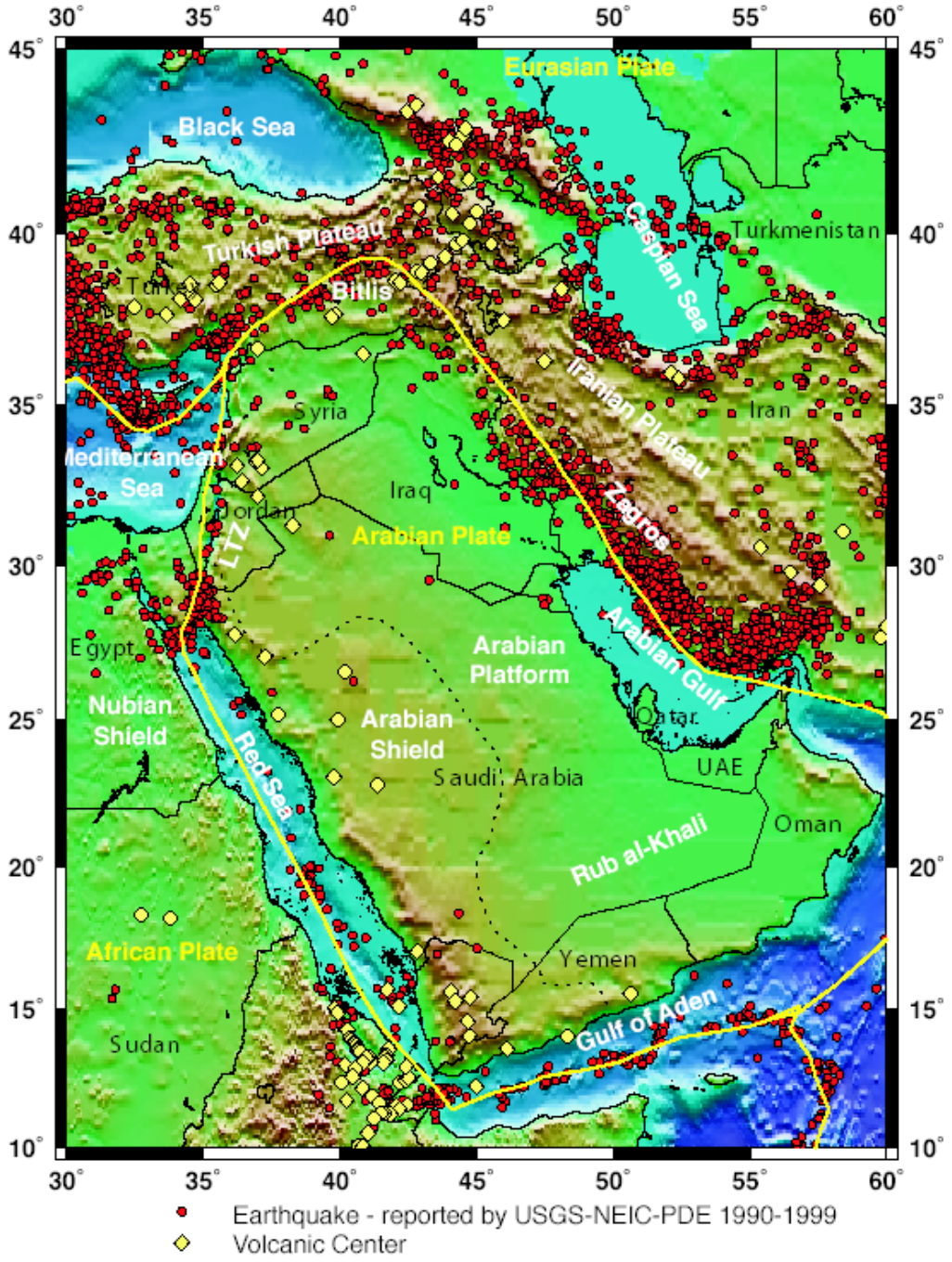

Figure 1. Map of the Arabian Peninsula and surrounding regions. Major geographic and tectonic/geologic features are indicated. Plate boundaries are indicated by yellow lines. Earthquakes and volcanic centers are shown as red circles and yellow diamond, respectively.

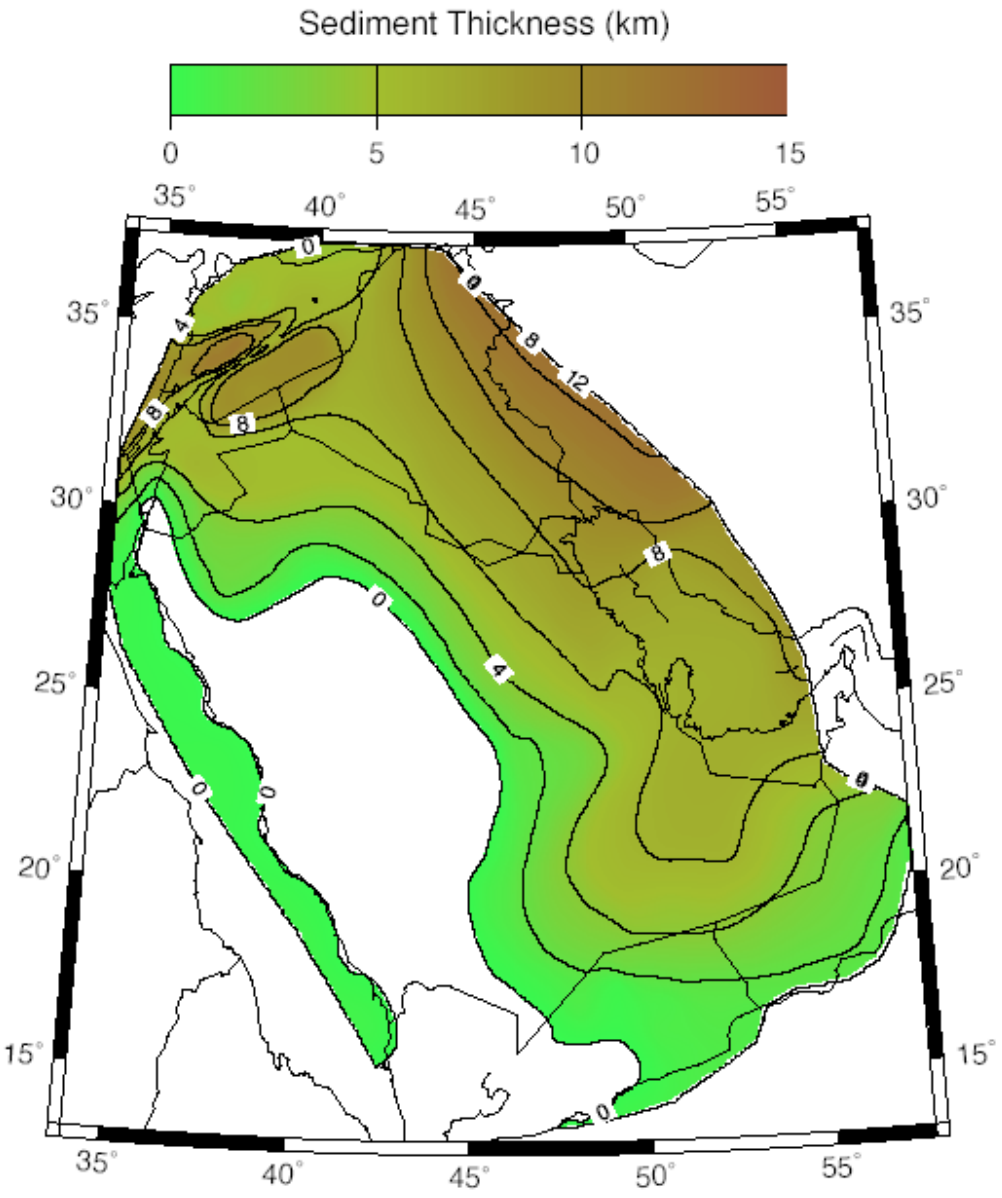

Figure 2. Map of sediment thickness of the Arabian Plate.

related to the opening of the Red Sea and mantle asthenospheric upwelling beneath western Arabia (e.g. *Camp and Roobol*, 1992).

The northwestern regions of Saudi Arabia are distinct from the Arabian Shield, as this region is characterized by high seismicity in the Gulf of Aqabah and Dead Sea Rift. Active tectonics in this region is associated with the opening of the northern Red Sea and Gulf of Aqabah as well as a major continental strike-slip plate boundary.

The Dead Sea transform system connects active spreading centers of the Red Sea to the area where the Arabian Plate is converging with Eurasia in southern Turkey. The Gulf of Aqabah in the southern portion of the rift system has experienced left-lateral strike-slip faulting with a 110 km offset since early Tertiary to the present. The seismicity of the Dead Sea transform is characterized by both swarm and mainshock-aftershock types of earthquake activities. The instrumental and historical seismic records indicate a seismic slip rate of 0.15-0.35 cm/year during the last 1000-1500 years, while estimates of the average Pliocene-Pleistocene rate are 0.7-1.0 cm/year.

Historically, the most significant earthquakes to hit the Dead Sea region were the events of 1759 (Damascus), 1822 (Aleppo), and of 1837 ;1068 (Gulf of Aqabah area) caused deaths of more than 30,000 people. *Ben Menahem* (1979) indicated that about 26 major earthquakes ($6.1<ML<7.3$) occurred in southern Dead Sea region between 2100 B.C. and 1900 A.D. In 1980's and 1990's, the occurrence of earthquake swarms in 1983, 1985, 1991, 1993 and 1995 in the Gulf of Aqabah clearly indicates that this segment is one of the most seismically active zones in the Dead Sea transform system. Earthquake locations provide evidence for continuation of faulting regime from the Gulf northeastward inland beneath thick sediments, suggesting that the northern portion of the Gulf is subjected to more severe seismic hazard compared to the southern portion (*Al-Amri et al*.,1991).

To the south, the majority of earthquakes and tectonic activity in the Red Sea region are concentrated along a belt that extends from the central Red Sea region south to Afar and then east through the Gulf of Aden. There is little seismic activity in the northern part of the Red Sea, and only three earthquakes have been recorded north of latitude 25^{o} N. Instrumental seismicity of the northern Red Sea shows that 68 earthquakes (3.8<mb<6.0) are reported to have occurred in the period from 1964 to 1993.

Historically, about 10 earthquakes have occurred during the period 1913-1994 with surface-wave *(Ms)* magnitudes between 5.2 and 6.1. Some of these events were associated with earthquake swarms, long sequences of shocks and aftershocks (the earthquakes of 1941, 1955, 1967 and 1993). The occurrence of the January 11,1941 earthquake in the northwest of Yemen (*Ms = 5.9*) with an aftershock on February 4, 1941 *(Ms* = 5.2), the earthquake of October 17, 1955 *(Ms* = 4.8), and the 1982 Yemen earthquake of magnitude 6.0 highlight the hazards that may result from nearby seismic sources and demonstrate the vulnerability of northern Yemen to moderate-magnitude and larger earthquakes. Instrumental seismicity of the southern Red Sea shows that 170 earthquakes (3.0<*mb*< 6.6) are reported to have occurred in the period 1965-1994. The historical and instrumental records of strong shaking in the southern Arabian Shield and Yemen (1832; 1845; 1941; 1982 and 1991) indicate that the return period of severe earthquakes which affect the area is about 60 years (*Al-Amri*,1995 b).

The Arabian Plate boundary extends east-northeast from the Afar region through the Gulf of Aden and into the Arabian Sea and Zagros fold belt. The boundary is clearly delineated by teleseismic epicenters, although there are fewer epicenters bounding the eastern third of the Arabian Plate south of Oman. Most seismicity occurs in the crustal part of the Arabian Plate beneath the Zagros folded belt (*Jackson and Fitch*,1981). The Zagros is a prolific source of large magnitude earthquakes with numerous magnitude 7+ events occurring in the last few decades. The overall

lack of seismicity in the interior of the Arabian Peninsula suggests that little internal deformation of the Arabian Plate is presently occurring.

Seismic structure studies of the Arabian Peninsula have been varied, with dense coverage along the 1978 refraction survey and little or no coverage of the aseismic regions, such as the Empty Quarter. In 1978, the Directorate General of Mineral Resources of Saudi Arabia and the U.S. Geologic Survey conducted a seismic refraction survey aimed a determining the structure of the crust and upper mantle. This survey was conducted primarily in the Arabian Shield along a line from the Red Sea to Riyadh. Reports of crust structure found a relatively fast velocity crust with thickness of 38-43 km (*Mooney et al*,1985; *Mechie et al*,1986; *Gettings et al*,1986, *Badri*,1991). The crust in the western shield is slightly thinner than that in the eastern shield.

Mooney et al.(1985) Suggest that the geology and velocity structure of the Shield can be explained by a model in which the Shield developed in the Precambrian by suturing of island arcs. They interpret the boundary between the eastern shield and the Arabian Platform as a suture zone between crustal blocks of differing composition.

Surface waves observed at the long-period analog stations RYD (Riyadh), SHI (Shiraz, Iran), TAB (Tabriz, Iran), HLW (Helwan, Egypt), AAE (Addis-Ababa, Ethiopia) and JER (Jerusalem) were used to estimate crustal and upper mantle structure (*Seber and Mitchell*, 1992; *Mokhtar and Al-Saeed*,1994). These studies reported faster crustal velocities for the Arabian Shield and slower velocities for the Arabian Platform.

The Saudi Arabian Broadband Deployment (*Vernon and Berger et al*., 1997; *Al-Amri et al.,* 1999) provided the first data set of broadband recordings of this region. This deployment consisted of 9 broadband three-component seismic stations along a similar transect an early seismic refraction study (*Mooney et al., 1985; Gettings et al.,1986; Mechie et al.,*1986). Data from the experiment resulted in several studies andd models (*Sandvol et al.,* 1998; *Mellors et al.,*

1999; *Rodgers et al.,* 1999; *Benoit et al.,* 2002). These studies provided new constraints on crustal and upper mantle structure. The crustal model of the western Arabian Platform shows a little higher P-velocity for the upper crust in the Shield than in the Platform and the crustal Platform seems to have a greater thickness than in the Shield by about 3 km. The Moho discontinuity beneath the western Arabian Platform indicates a velocity of 8.2 km/sec of the upper mantle and 42 km depth (*Al-Amri,*1998;1999).

Generally the crustal thickness in the Arabian Shield area varies from 35 to 40 km in the west adjacent to the Red Sea to 45 km in central Arabia (*Sandvol et al.,* 1998; *Rodgers et al.,* 1999). Not surprising the crust thins nears the Red Sea (*Mooney et al.,*1985; *Gettings et al.,*1986; *Mechie et al.,*1986). High-frequency regional S-wave phases are quite different for paths sampling the Arabian Shield than those sampling the Arabian Platform (*Mellors et al.,* 1999; *Sandvol et al.,*1998). In particular the mantle Sn phase is nearly absent for paths crossing parts of the Arabian Shield, while the crustal Lg phase is extremely large amplitude. This may result from an elastic propagation effect or extremely high mantle attenuation and low crustal attenuation occurring simultaneously, or a combination of both.

Previous reports of large scale seismic structure (e.g. *Ritsema et al.,*1999 and *Debayle et al.,*2001) suggest that a low velocity anomaly in the upper mantle extends laterally beneath the Arabian Shield from the Red Sea in the west to the shield – platform boundary in the east. Additionally, *Debayle et al*. (2001) observe a narrow region of low velocity beneath the Red Sea and western edge of the Arabian Shield, extending to 650 km depth. A recent tomographic velocity model and receiver function analysis by *Benoit et al.* (2002) suggests the upper mantle low velocity anomaly is smaller in extent, laterally and vertically, than imaged in previous studies.

3. SEISMOGRAPHIC NETWORKS IN SAUDI ARABIA

There are two independent analog seismic telemetry networks in Saudi Arabia. King Saud University (KSU) network features 31 stations. King Abdulaziz City for Science and Technology (KACST) operates a network of three-component broadband and short-period stations (*Al-Amri and Al-Amri*, 1999). Both networks have stations throughout the Kingdom of Saudi Arabia, but the station density is greatest near the Gulf of Aqabah. These networks recorded the shots with good signal-to-noise above about 0.5 Hz.

Recently, KSU and KACST networks run the Boulder Real Time Technologies (BRTT) Antelope System as described below.

ANTELOPE is a system of software modules that implement acquisition, transport, buffering, processing, archiving and distribution of environmental monitoring information. Antelope is a distributed, open-architecture, UNIX-based acquisition, analysis and management system. It consists of two major sub-systems, namely Antelope Real Time System **(ARTS)** and Antelope Seismic Information System **(ASIS)**.

ARTS brings raw data from remote field sites in real time to KSU processing center where, automated real time processing of data is performed and information is automatically merged into long term information system archives. Within ARTS, data is buffered and transported through a mechanism known as an Object Ring Buffer **(ORB)**, which acts as the heart of ARTS. The ORB is managed by a single program, "*obrserver"*. Field interface modules write all of the data from the field stations into the ORB. The concepts behind an ORB are straightforward:

1) A circular raw data store on disk

2) A server-client approach to manage the circular data store

3) All server-client inter-process communications take place through Internet sockets using TCP/IP.

Real time Richter magnitude estimates are made by a module called "*orbmag*". This program looks for ASIS origin rows data in the data processing ORB. For each origin read, *orbmag* determines appropriate time windows for each station and acquires the waveform data for all components from the same data processing ORB. Each waveform segment is converted to equivalent drum recorder displacement of a standard Wood-Anderson instrument and the maximum amplitude for the event is determined. These amplitudes are fed into the standard Richter magnitude formula for computing ml values for each station and all of the station ml values are median averaged to get a total network ml estimate. The *ml* estimate is used to modify the input origin row and this modified origin row is written back into the data processing ORB.

Location capability is provided by program "*orbgenloc*" which uses traditional inversion algorithm. The program "*orbenloc*" provides a generic location capability using traditional inversion algorithms. In addition, locations produced by "*orbassoc*" module can be fine tuned with "*orbgenloc*". "*orbgenloc*" reads the arrival, association and preliminary hypocenter information produced by "*orbassoc*" and computes a more refined earthquake location using a variety of traditional inversion algorithms. The refined locations are written to an output ORB as database row packets.

3.1 KSU Seismographic Network

The King Saud University (KSU) seismological network was established in 1985 and includes the digital WWSSN station in Riyadh. Currently, the network consists of 31 stations with denser sub-networks in the Gulf of Aqabah region (12 stations) and the southwestern part of Saudi Arabia (8 stations). The seismographic station in Riyadh is a 6 - channel station and consists of

three S-13 short-period and three SL-200 long-period seismometers. The seismometer outputs are amplified, filtered and recorded in both analog and digital form. The filters allow recording in four different periods (SP wide band, SP narrow band, LP wide band and LP narrow band). The total system response for the Riyadh station is broadband (0.01 to 33 Hz). Signals from the 9 channels are also routed to a 12-bit A-to-D converter and recorded on 9-track magnetic tape. The other telemetered seismic stations are equipped with S-13 short-period seismometers connected to a field case housing an amplifier, a voltage controlled oscillator (VCO), an automatic daily calibrator and a telemetry interface.

3.2 KACST Seismographic Network

In May 1998 King Abdulaziz City for Science and Technology (KACST) began operating the Saudi Arabian National Digital Seismic Network (SANDSN). A description of the SANDSN is given in *Al-Amri and Al-Amri* (1999). It consists of 38 stations mostly distributed across the Arabian Shield (western Saudi Arabia, Figure 3). The instrumentation features 27 broadband and 11 short-period instruments. The station information is compiled in Table 1. All stations record three-component ground motions at a sample rate of 100 samples/second. The stations operate continuously and transmit data in real-time to the KACST Headquarters building in Riyadh. The KACST Data Center receives the raw waveform data and runs the Boulder Real Time Technologies (BRTT) Antelope System. This is a software package for managing real-time seismic network data and performing the basic network operations of detection, association and location of events as well as data archival. A short-term average-to-long-term average (STA/LTA) energy detector runs continuously and detects phase arrivals. The system attempts to locate the event if a number of arrivals are detected by the network within a specified time window. The system locates events relative to a single average global velocity model (*iasp91*,

Kennett and Engdahl, 1991). This is a global continental average velocity model derived from worldwide observations of seismic travel times. While this model is appropriate for locating distant events, it is not necessarily a good model for locating events in and around the Arabian Peninsula. Figure 4 shows the iasp91 model along with lithospheric velocity models from our earlier work (*Rodgers et al*., 1999; *Rodgers et al*., 2001). As one can see *iasp91* has no sediment layer and the crustal thickness (35 km) is thin compared to the Arabian Platform model. There are also differences between the mantle velocities. We will return to these issues below.

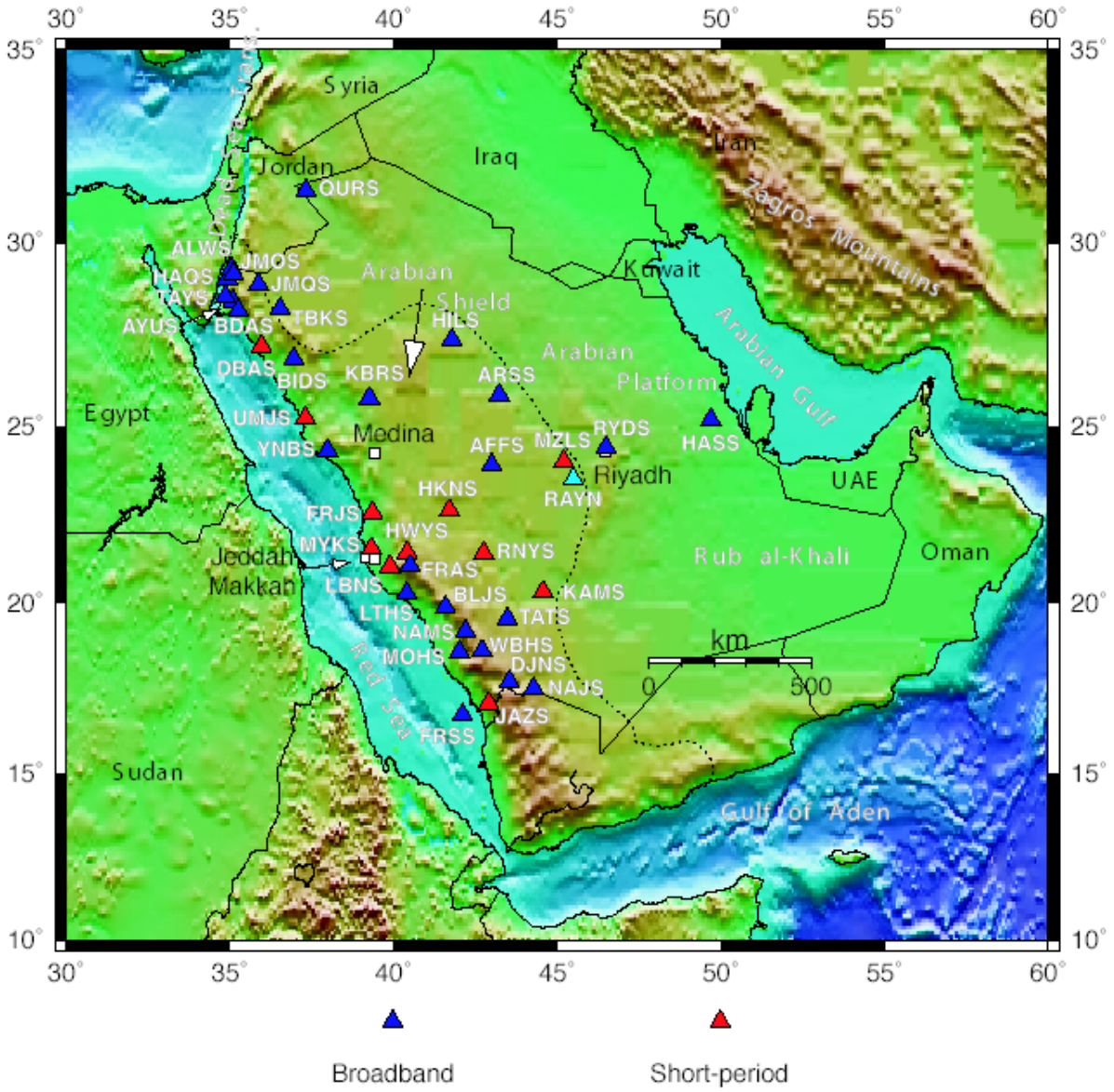

Figure 3. Map of the stations from the Saudi Arabian National Digital Seismic Network (SANDSN).

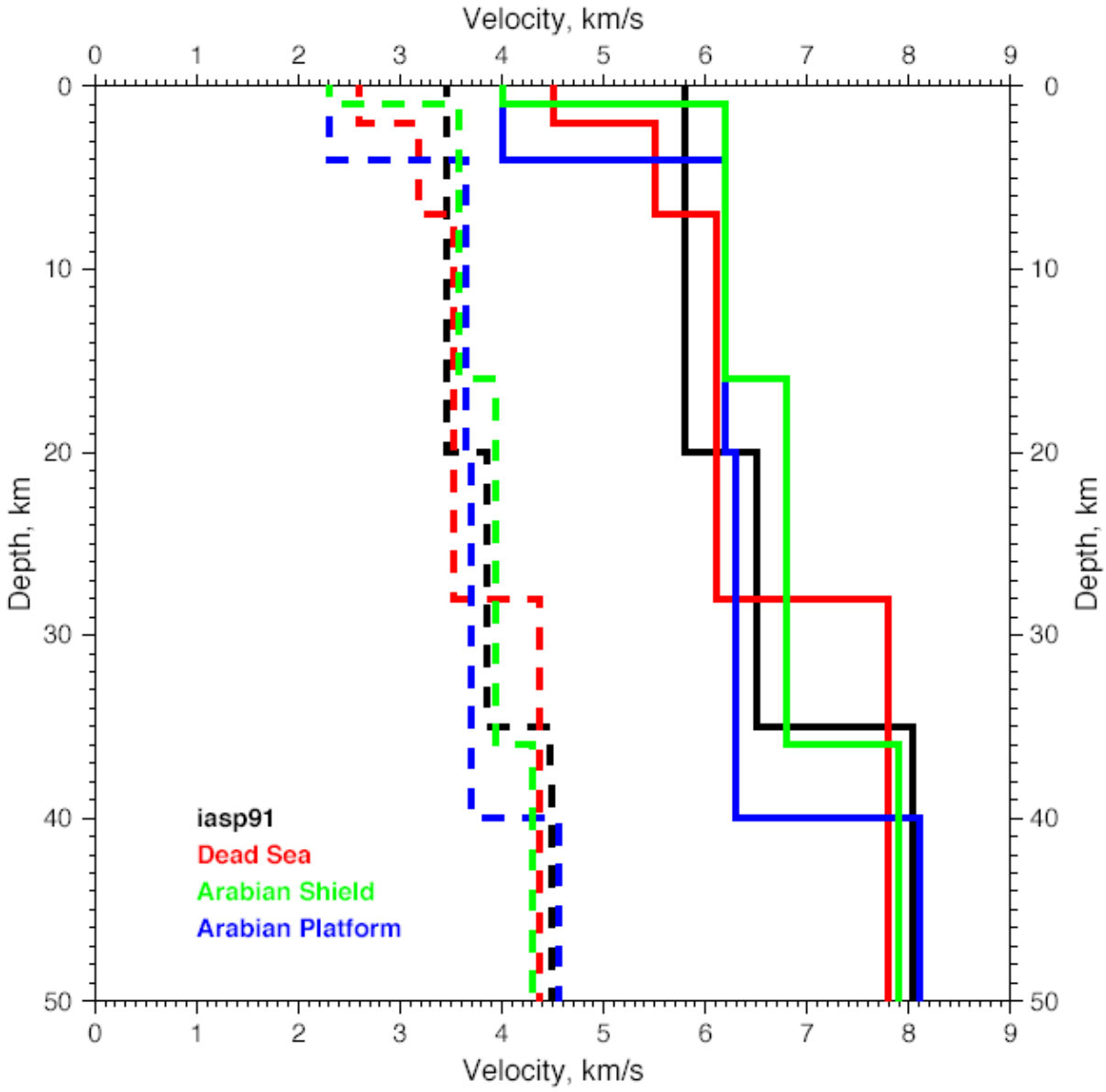

Figure 4. Seismic P- and S-wave velocity models, solid and dahsed respectively, for the Arabian Peninsula from various sources described in the text.

Table 1. Stations of the Saudi Arabian National Digital Seismic Networok (SANDSN).

Station Code	Station Location	Latitude	Longitude	Elevation (meters)	Sensor Type
AFFS	Afif	23.9267	43.0005	109	BB
ALWS	As Safayhah	29.3103	35.0650	0	SP
ARSS	Ar Rass	25.8810	43.2365	72	BB
AYUS	Aynunah	28.1889	35.2689	0	SP
BDAS	Al Bada	28.4317	35.1014	36	BB
BIDS	Al Bida	26.8670	36.9595	0	BB
BLJS	Baljurashi	19.8812	41.5992	206	BB
DBAS	Duba	27.2114	35.9773	18	SP
DJNS	Dahran-Al-Janub	17.7073	43.5434	220	BB
FRAS	Faraa	21.0622	40.5200	0	BB
FRJS	J.-Farasan	22.5905	39.3638	0	SP
FRSS	Farasan Island	16.7392	42.1143	0	BB
HAQS	Haql	29.0548	34.9297	42	BB
HASS	Al Hasa	25.1899	49.6944	20	BB
HILS	Al Hail	27.3835	41.7917	108	BB
HKNS	J.-Hakran	22.6420	41.7158	0	SP
HWYS	Hawiyah	21.4349	40.4177	0	SP
JAZS	Jizan	17.0678	42.9177	0	SP
JMOS	J. Al-Moallq	29.1686	35.1094	0	BB
JMQS	J. Al-Moqyreh	28.8861	35.8778	0	BB
KAMS	Al Khamasin	20.3092	44.5798	75	SP
KBRS	Harrat Khaybar	25.7893	39.2623	78	BB
LBNS	J. Laban	21.0465	39.9013	0	BB
LTHS	Al Lith	20.2750	40.4107	18	BB
MOHS	Muhayl	18.5761	42.0190	52	BB
MYKS	Mirrayikh	21.5545	39.3323	0	SP
MZLS	Mezel	24.0275	45.2071	88	SP
NAJS	Najran	17.5034	44.2847	131	BB
NAMS	Namsa	19.1714	42.2084	252	BB
QURS	Al Hadithat	31.3860	37.3240	49.1	BB
RNYS	Wadi Ranyah	21.4267	42.7662	0	SP
RYDS	Riyadh	24.1900	46.6400	0	BB
TATS	Tathlith	19.5412	43.4775	110	BB
TAYS	Tayyib Ism	28.5511	34.8717	0	BB
TBKS	Tabuk	28.2248	36.5485	82	BB
UMJS	Umm Lajj	25.2340	37.3119	13	SP

WBHS	Wadi-Ibnhashbal	18.6057	42.7144	187	SP
YNBS	Yanbu	24.3397	37.9922	8	BB

3.3 GSN Seismic Station

RAYN is one of the newest stations in the IRIS/IDA global seismographic network. The seismic station at Ar Rayn (RAYN), Saudi Arabia was established in 1996 under a memorandum of understanding between KACST, the IRIS Consortium, and the University of California, San Diego (UCSD), with key support from the KSU Department of Geology.

RAYN station consists of a STS-2 three-component broadband seismometer (passband between 0.008 Hz and 50 Hz), a Kinemetrics FBA-23 strong motion accelerometer, and a Teledyne broadband KS-54000 (passband between 0.0003 Hz and 8 Hz). The KS-54000 is emplaced in a borehole at a depth of 100 meters to insure the quietest possible recording environment. The purpose of installing the STS-2 is to provide much better coverage of high frequencies than would be possible with the KS-54000 alone. The FBA-23 is in place to record ground motion from earthquakes either too large or too close to be recorded on-scale by the KS-54000 and STS-2. All sensors are recorded on an IRIS-3 high-resolution data acquisition system.

The IRIS/IDA station RAYN has noise characteristics which place it among the quietest seismic stations in the world. Minimum detectable magnitudes are estimated for RAYN station using the observed noise levels over 1 Hz. The m_b detection threshold for the distance range of 5 -10 degrees is about m_b = 2.7-3.0 assuming the signal-to-noise ratio of 3 dB or better.

4. METHODOLOGY

We improved earthquake location and magnitude estimates using waveform data from the Saudi Arabian National Digital Seismic Network (SANDSN). The proposed research includes standard seismological investigations as well as newly developed techniques as follows :

4.1 Data Collection and Validation

The investigators wrote software to extract waveform data from the SANDSN data archive. This software facilitated the extraction and exchange of seismic waveform and parameter data.

In order to validate the station timing and instrument response we performed comparisons of timing and amplitudes of P-waves for large teleseismic events at the SANDSN stations with the Global Seismic Station RAYN. This station has well calibrated timing and instrument response. The relative arrival times of teleseismic P-waves at the SANDSN can be accurately measured by cross-correlating with the observed waveforms at RAYN and correcting for distance effects. Absolute amplitudes of teleseismic P-waves at the SANDSN and RAYN stations were measured by removing the instrument response and gain and band-pass filtering.

This study also considered many events and computed average travel time and amplitude residuals relative to a globally averaged one dimensional earth model, such as iasp9l. Although there were deviations between the timing and amplitudes of SANDSN P-waves from the predictions of the iasp9I model (because of lateral heterogeneity) the tests were useful to identify which stations might have timing and / or instrument calibration problems.

4.2 Travel Time Calibration

One of the most fundamental elements of seismological research is earthquake location. In fact the main product of any seismic network is the reporting of earthquake location, origin time and

magnitude. The first major element of our proposed research is to improve earthquake locations by developing and improving models of the seismic velocity structure. It is well known that the lithosphere (crust and uppermost mantle) of Saudi Arabia is heterogeneous. Some of the difference in the seismically inferred crustal structure of eastern and western Arabia is due to the thick sediments of the Arabian Platform. However, recent waveform modeling results (*Rodgers et al.,* 1999) suggest that there are also differences in the seismic velocities of the crystalline crust between the Arabian Shield and Platform. These differences result in travel time variations within the Arabian Peninsula, which will bias earthquake locations when a single, one - dimensional velocity model is used.

Similarly, variations in the amplitudes of regional phases, such as those reported by *Mellors et al*. (1999). That study reported that Pn, Pg and Sn body-waves from the Gulf of Aqabah events to central Arabia are weak, while Lg along is strong. More normal continental energy partitioning of the regional phases is observed for earthquakes from the Zagros. These variations in regional phase propagation characteristics can make it difficult to develop detection algorithms for regional phases, most importantly the first arriving Pn phase. The fundamental travel time and amplitude behavior of regional phases needs to be characterized before the SANDSN can be tuned to provide optimal phase detection, locations and magnitudes.

Accordingly, we improved earthquake location and origin time estimates by developing and improving models of the regional seismic phases and the seismic velocity structure of the lithosphere. Firstly, we collected data from large well-observed earthquakes with well-constrained locations, depths and origin times. Events with 50 or more observations (stations) and an open-azimuth of less than 90 degrees are typically located to within 20 km of ground truth locations as reported by *Sweeney* (1996). We used similar criteria to select well-located events for travel time analysis. Travel time picks of regional phases Pn, Pg, Sn and Lg were

reviewed by an analyst and quality controlled before they are included into the data set. Travel time curves for each phase were generated. As sufficient data are collected, we developed regional travel time models for different paths (e.g. Arabian Shield and Arabian Platform) and for events in different source regions (e.g. Gulf of Aqabah, Red Sea, Zagros Mountains).

4.3 Focal Mechanism Solutions, Moments and Refinement of Velocity Models

In order to develop a robust magnitude scale, earthquake moments, focal mechanisms and depths were estimated by modeling observed long-period three-component waveforms (*Walter* 1993). We modeled the observed waveforms with complete reflectivity synthetic seismograms (*Randall*,1994) using an appropriate seismic velocity model of the crust and shallow mantle. We first validated the current models (*Rodgers et al*.,1999), possibly refine them or develop new models. Special efforts were spent to define the regions of validity of the velocity models.

We began by first considering large earthquakes (Mw> 5.0) that are within regional distance (< 1500 km) of Saudi Arabia. Often events of this size have focal parameters from global observations (such the Harvard CMT or USGS-NEIC moment tensor projects).Waveform data for these events were selected and reviewed for signal-to-noise. The data were corrected for instrument response, converted to ground displacement and the horizontals were rotated to radial and transverse components.

Earthquake focal mechanism, depth and seismic moment were estimated by fitting synthetic seismograms to the long-period three-component waveforms. The source parameters are estimated by a grid search method (*Walter*,1993). For a series of depths, all possible orientations of the double couple focal mechanism (strike, dip and rake) are investigated.

5. RESULTS & DATA ANALYSIS

5.1 Seismic Noise Measurements

Background seismic noise is an unavoidable problem in earthquake monitoring. The amplitudes of seismic arrivals decrease with distance and seismic magnitude. Path propagation effects, such as attenuation and elastic structure lead to variability in seismic amplitudes. Noise inhibits the detection of weak seismic arrivals (phases) from distant and/or small events. Seismic noise is generated from a variety of sources. These include both man-made (e.g. roads, machinery) and natural sources (e.g. wind, ocean waves, temperature effects). Noise properties can vary between daylight and night hours and between seasons (e.g. summer and winter). Also the geologic character of the seismometer placement has great effect on the noise–hard rock sites typically have lower noise levels than sites on weathered or sedimentary rock or unconsolidated material. Because of the variety of noise sources and the variability of noise, propagation and site characteristics at network sites, the noise properties at seismic stations are frequency dependent and can be highly variable between sites.

Noise spectra were measured at stations AFFS, HASS, HILS, QURS and TATS of the SANDSN network. Stations were selected to be distributed around the Kingdom. Event-segmented data were previewed and first-arriving P-waves were picked. Waveforms were instrument corrected to absolute ground motion using the LLNL developed Seismic Analysis Code (SAC). Noise segments were taken as the available waveform before the P-wave pick. Typically for SANDSN data this was 30-60 seconds. For noise spectral measurements we accepted only segments 30 seconds or longer. This limited the low frequency resolution of our noise estimates. Power spectral densities were computed for noise windows by fast Fourier transform (FFT) and

normalized by the window length. Noise spectra are presented in acceleration in decibels relative 1 $(m/s^2)^2/Hz^2$.

Results for noise at SANDSN stations are presented in Figures 5-9. Shown in each plot are the vertical, north and east component noise acceleration power spectra (in decibels relative to 1 m^2/s^4). Also shown are the average low and high noise spectra of *Peterson* (1993). Results show that stations AFFS, HILS and TATS have the lowest noise levels. Stations HASS and QURS have the highest noise levels of the sites considered. Cultural noise appears as spikes in the power spectra at frequencies above 1 Hz. This is most notable at stations HILS (4 and 8 Hz) and QURS. These sites may be affected by nearby cultural noise sources, such as roads and human activities.

Generally, the noise is relatively low amplitude between 0.1 and 1 Hz, except for station HASS. Detection of energy at frequencies around 1 Hz is most important for P-wave arrivals used in the event location. Higher frequency energy is useful for detecting local and regional events, less than 1000 km away.

5.2 SANDSN Location Performance

One of the fundamental tasks of a seismic network is to locate events. However one of the outstanding challenges of earthquake monitoring is to estimate accurate event locations. This is caused by several factors most important among them are insufficient sampling and inaccurate seismic velocity models. National borders and limited data sharing between institutions often inhibit the geographic sampling of any given seismic event. In particular accurate event location is very difficult when the event is not surrounded by the locating network – as often happens when the event is on or outside national borders. This problem is particularly acute for Saudi Arabia where the seismicity lies on the tectonic plate boundaries that surround the country on all

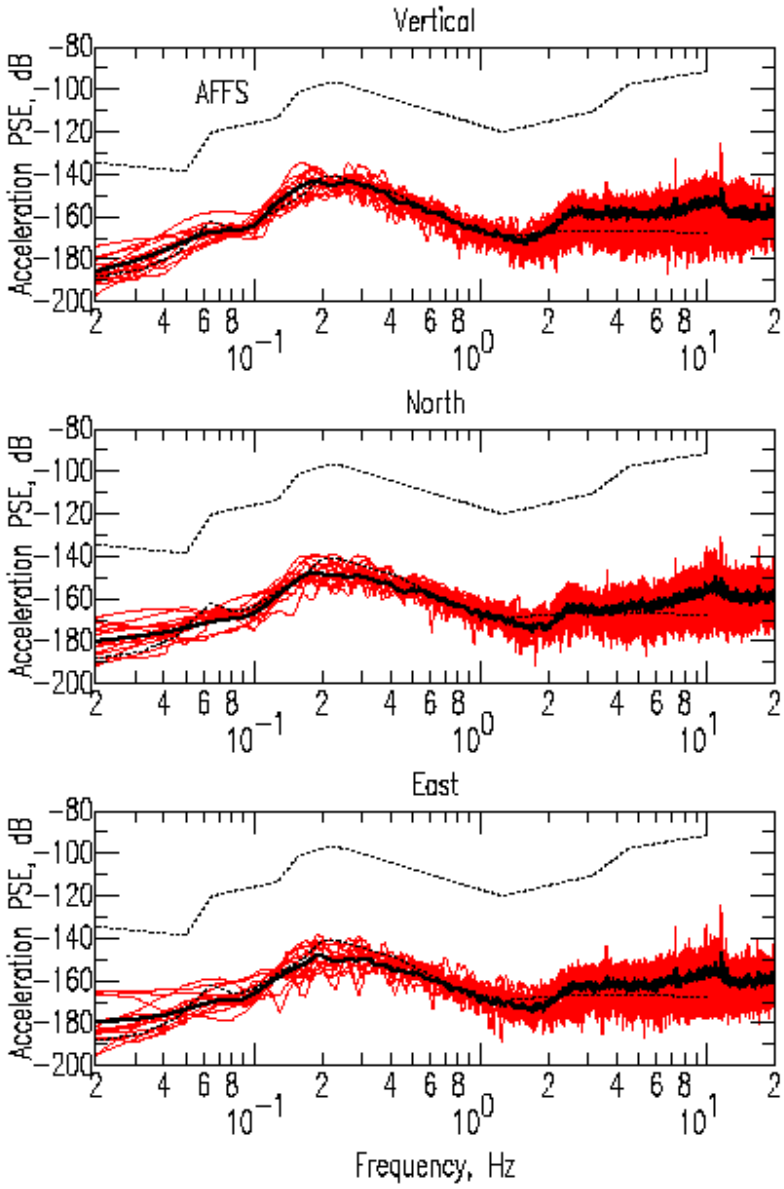

Figure 5. Noise spectra at station AFFS. Acceleration power spectra (in decibels relative to 1 m^2/s^{-4}) are shown for the vertical, north and east components. Individual spectra are shown in red and the average spectra in black. Also shown are the average low and high noise spectra (dotted line) of Peterson (1993).

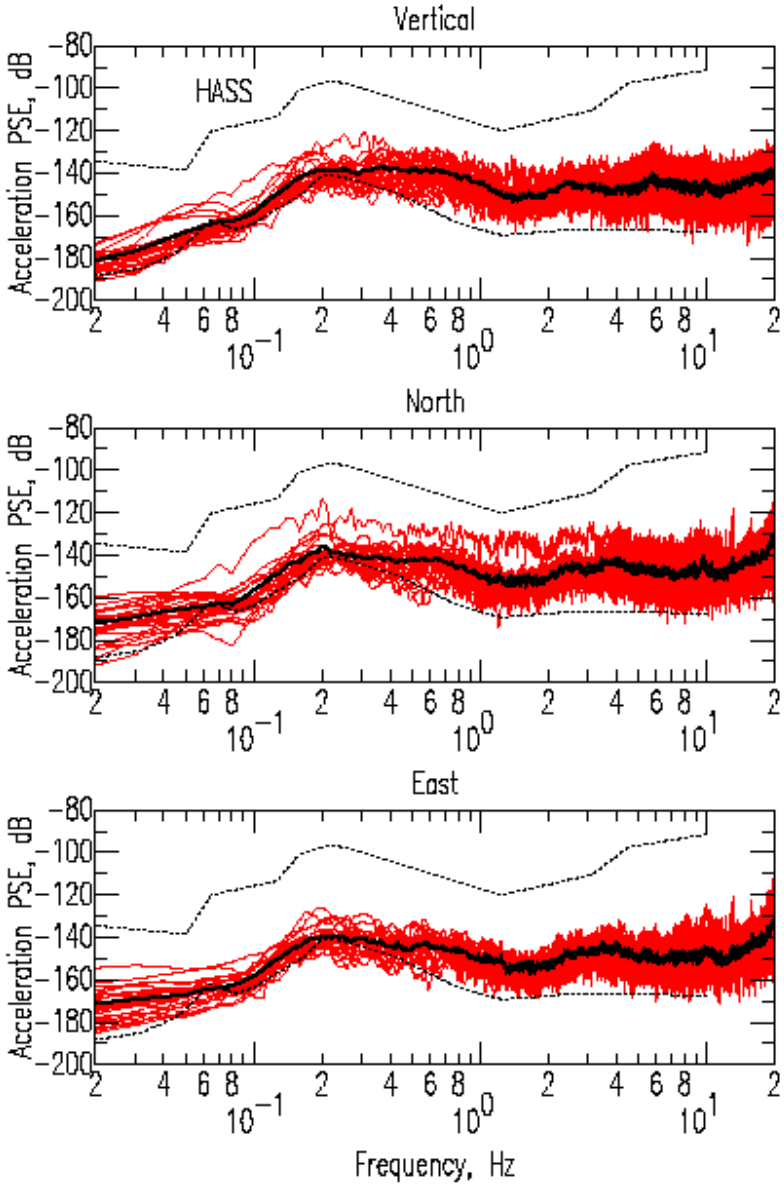

Figure 6. Noise spectra at station HASS, similar to Figure 5.

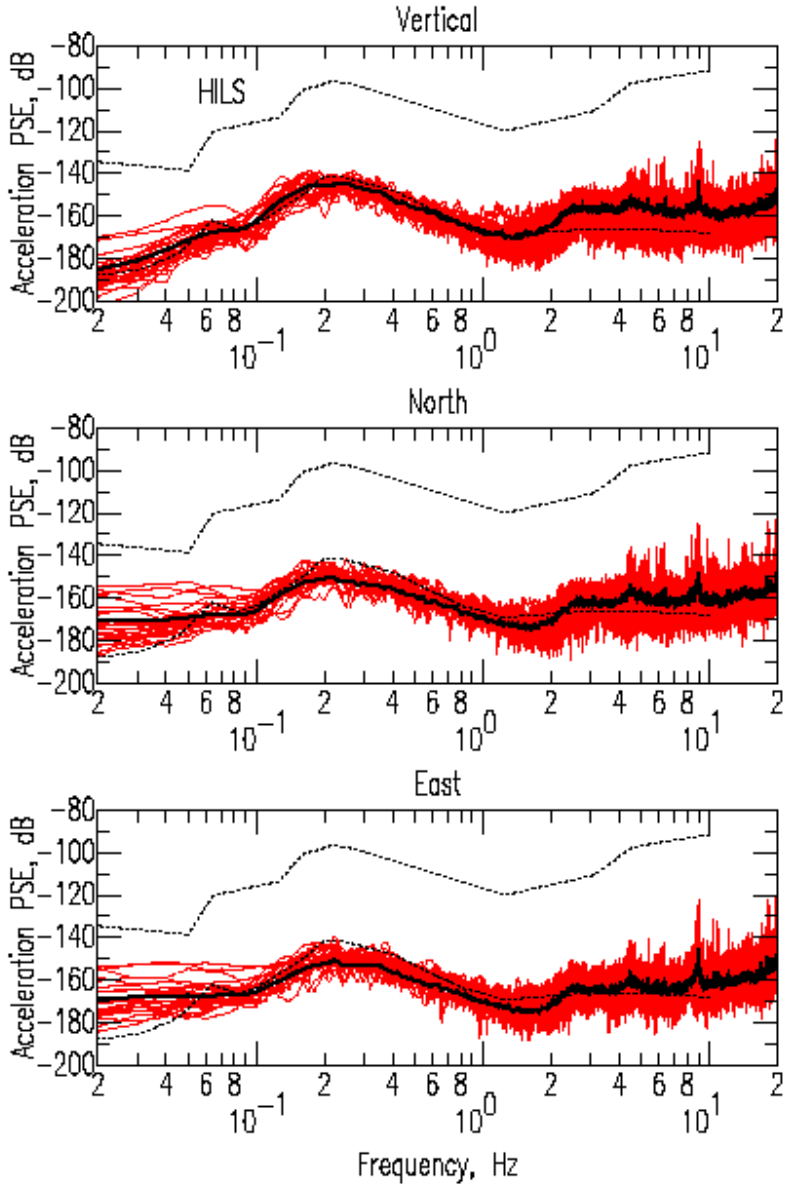

Figure 7. Noise spectra at station HILS, similar to Figure 5.

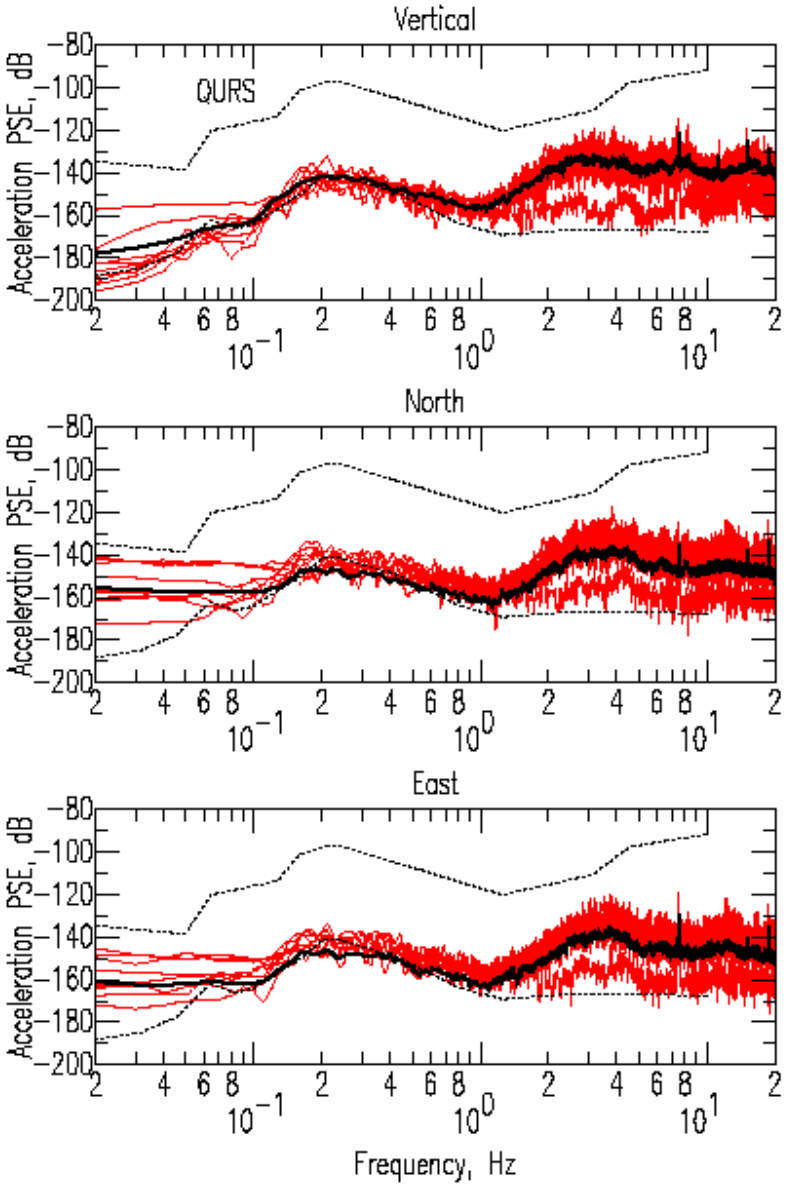

Figure 8. Noise spectra at station QURS, similar to Figure 5.

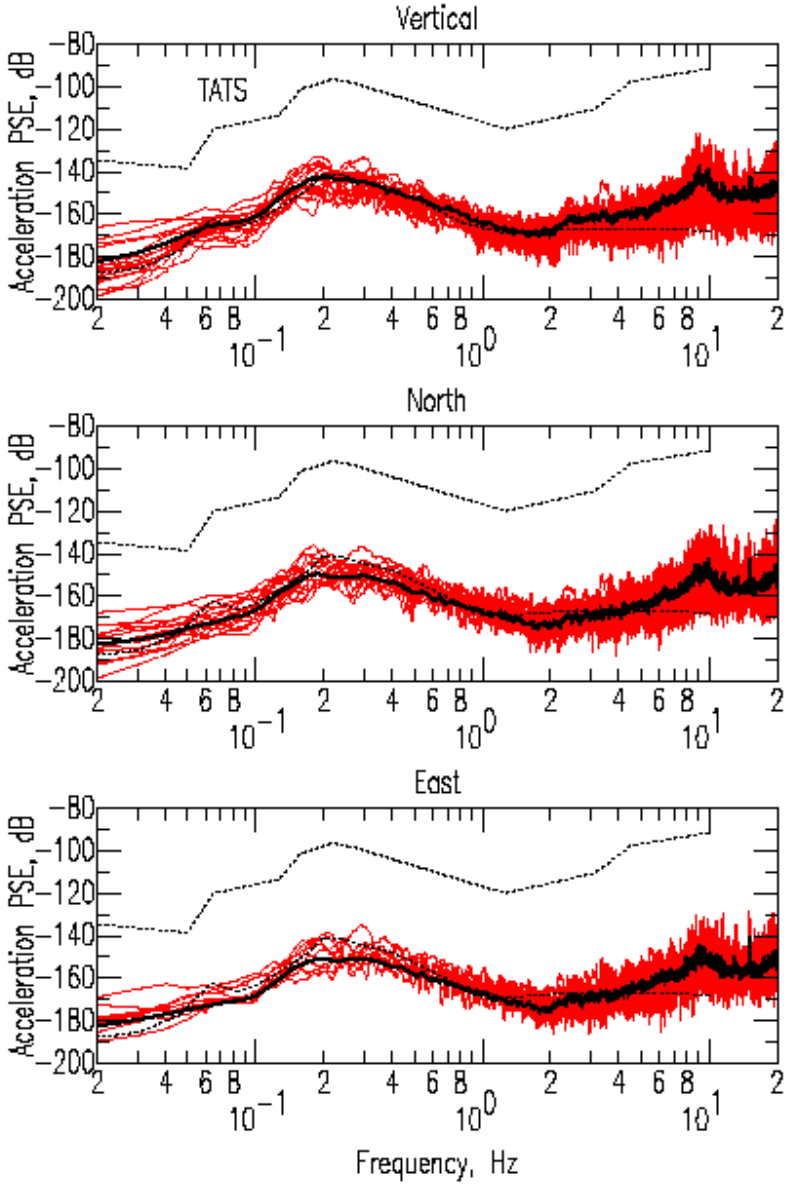

Figure 9. Noise spectra at station TATS, similar to Figure 5.

sides (Red Sea, Gulf of Aqabah / Dead Sea Transform system, Bitlis suture, Zagros Thrust, Makran, and Gulf of Aden).

However, one can improve locations of events outside the network by calibrating the travel times or velocity structure between the event regions and recording stations. The arrival times of moderate-sized events ($m_b \geq 4.5$) can be accurately measured to uncertainties of 1 second or less, if noise levels allow for good signal-to-noise levels. The calibration task is made difficult by the fact that one often does not accurately know the location and origin times of events. Events with accurate locations and origin times, so called ground truth (GT) events, are difficult to obtain. GT events come in various varieties. Man-made explosions with controlled location and detonation time are the best and most difficult to obtain form of ground truth. These events can be located with uncertainties of less than 100 meters and the origin times can be determined to tenths of a second. Mining and civil engineering explosions can be good sources of ground truth, however these events are often too small to be observed beyond 100 km. Earthquakes excite more seismic energy and can be observed at larger distances, however, their locations are poorly more constrained. In some cases where an earthquake is recorded at local distances (< 100 km) with good azimuthal coverage, the locations can be accurate to less than 10-20 km (*Sweeney,* 1996). This translates to 1-2 seconds of travel time at regional distances.

5.3 Comparison with Catalog Locations

Earthquake locations for events in and around Saudi Arabia were then compared with those reported by networks with global station coverage (e.g. REB, USGS-PDE and ISC). The comparison first associates events from each catalog in the LLNL Seismic Research Database. Event locations must occur at nearly the same time and location to be associated with the same

event. The global catalogs have the advantage of global azimuthal coverage of each event, while the SANDSN network has observations limited to stations within the Kingdom of Saudi Arabia. Most of the seismicity occurs near or outside the borders of the Kingdom, making location strongly dependent on the assumed seismic velocity model and travel time curve(s).

We chose to compare SANDSN locations with those reported by: the Provisional Technical Secretariat (PTS) of the Comprehensive Test Ban Treaty Organization (CTBTO) Reviewed Event Bulletin (REB); International Seismological Centre (ISC) and the United States Geological Survey (USGS) National Earthquake Information Center (NEIC) Preliminary Determination of Epicenters (PDE). These organizations report seismic event catalogs based on world-wide observations of body-wave arrival times.

We restricted the global catalog event magnitudes to be 4.0 or greater. This reduces small events that might be poorly observed and located by the global network(s). Figure 10 shows the comparison between the SANDSN and global catalog locations for the given dataset. The Dead Sea, Gulf of Aqabah and Zagros Mountains are the most seismically active regions around Saudi Arabia.

Figure 11 shows a map of SANDSN and global network locations for the Dead Sea/Gulf of Aqabah region. A statistical charcterization of the location differences, shown in Figure 12, indicates that the SANDSN locations are on average about 40 km different and to the southwest of the global catalog locations, although the location differences are highly scattered. The seismicity in this region are dominated by probable mine blasts in southern Jordan. These events are probably small and locations appear to be strongly biased to the southwest, however these differences could be due to location errors by in REB. Event locations in the Gulf of Aqabah are consistent with the global network locations.

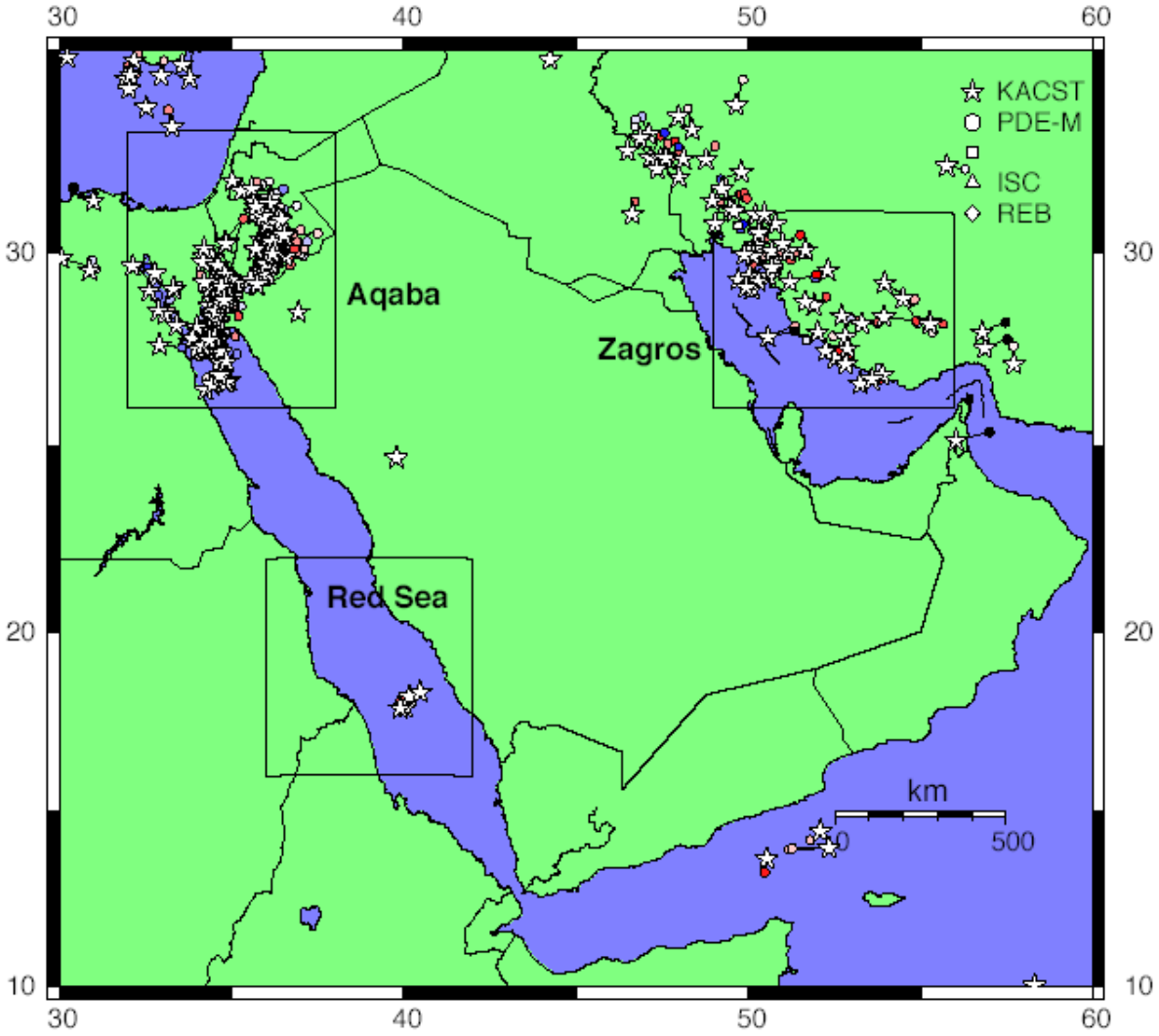

Figure 10. Comparison between SANDSN and global catalog locations for regions in and around Saudi Arabia. Sub-regions are identified by the boxes are analyzed in detailed.

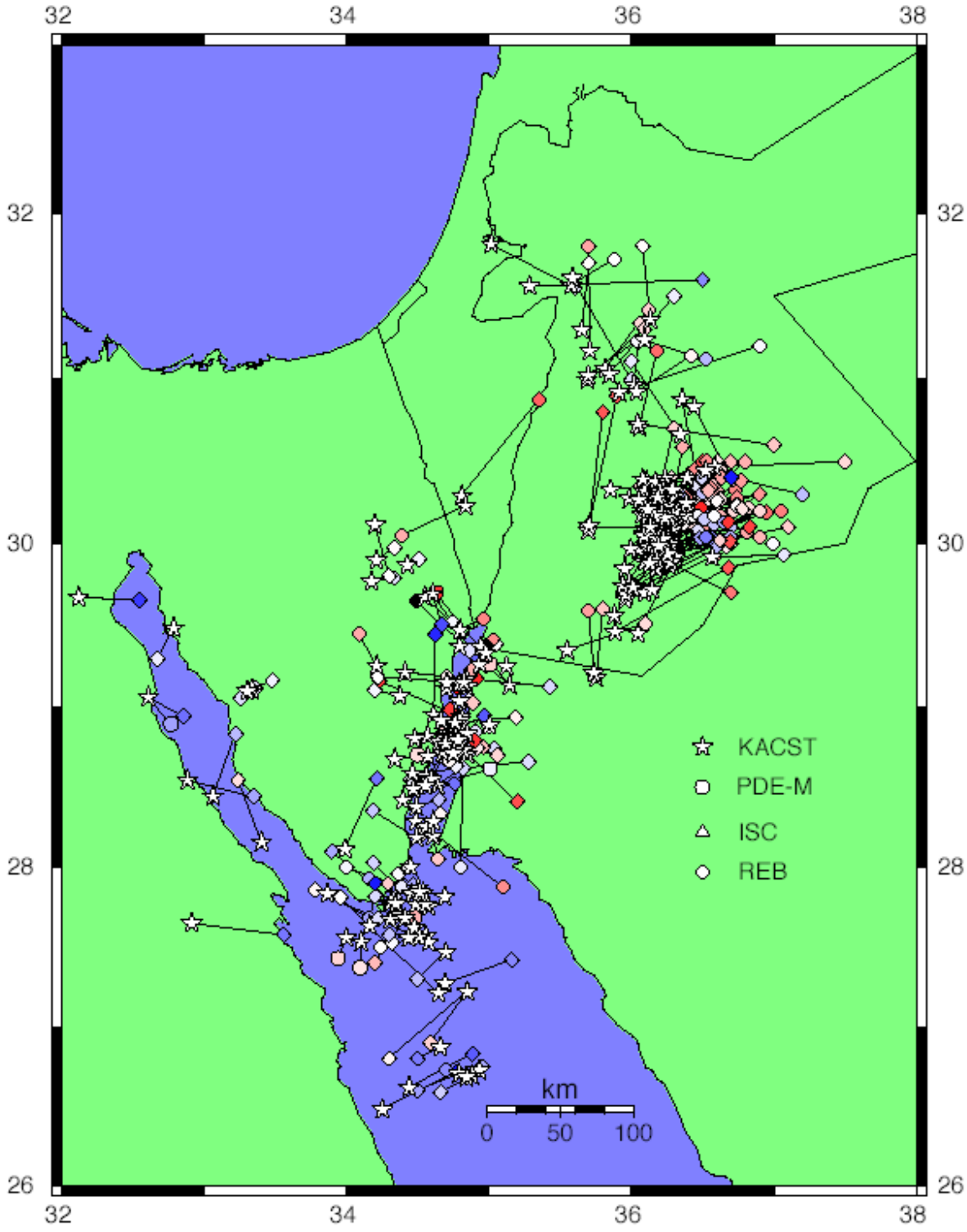

Figure 11. Comparison of SANDSN (stars) and global network locations (other symbols) for the Dead Sea/Gulf of Aqaba region. The color of the symbols for global network locations are scaled by the origin time difference.

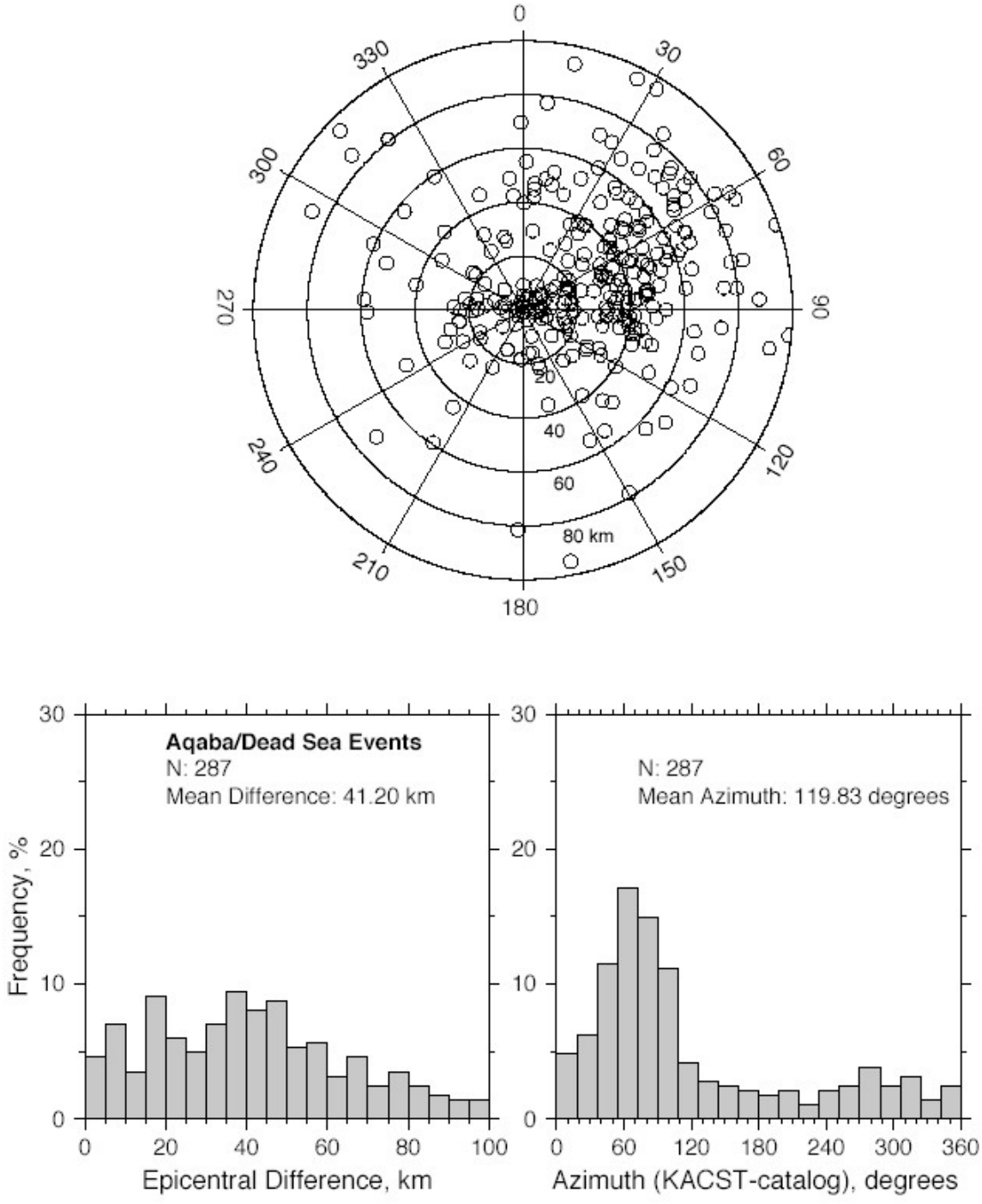

Figure 12. Statistical characterization of location differences between SANDNSN and global network locations for the Dead Sea/Gulf of Aqaba region: (top) azimuth and distance; (left) epicentral difference; (right) directional bias in locations.

Figure 13 shows the comparison of event locations from the SANDSN and global network bulletins for the Zagros Mountains region. The map shows that the SANDSN locations are generally to the southwest of the global network locations. This is also seen in a statistically analysis of the location differences, shown in Figure 14. The mean location (epicenter) difference is over 50 km. This corresponds to travel time error of as much as 6 seconds.

We preformed similar analysis on a very limited set of Red Sea events, shown in Figure 15. The location differences do not appear to be very large for the events studied. There are not many large events in this area.

These location differences are probably due to velocity model errors and can be reduced by using more appropriate region-dependent velocity models instead of the *iasp91* model. The *iasp91* model is a global average model for continental regions and is most accurate for predicting teleseismic travel times. At local to regional distances (0-1500 km) travels times are strongly region dependent due to lithospheric structure (i.e. crustal thickness, crustal and uppermost mantle seismic velocities and attenuation). These variations also lead to differences in regional phase amplitudes and propagation characteristics and require detailed study beyond the scope of the current project.

5.4 Improved Velocity Models for the Arabian Peninsula

In order to address the location performance issues detailed in the previous section, we have worked to develop improved models for the Arabian Peninsula. These models were developed using a variety of techniques, including travel time, waveform modeling and surface wave group velocity dispersion analysis. The models were developed for the major geologic/tectonic regions of Arabia: the Gulf of Aqabah/Dead Sea Region, the Zagros Mountains and the Arabian Shield. We used the best available data to estimate models for each region.

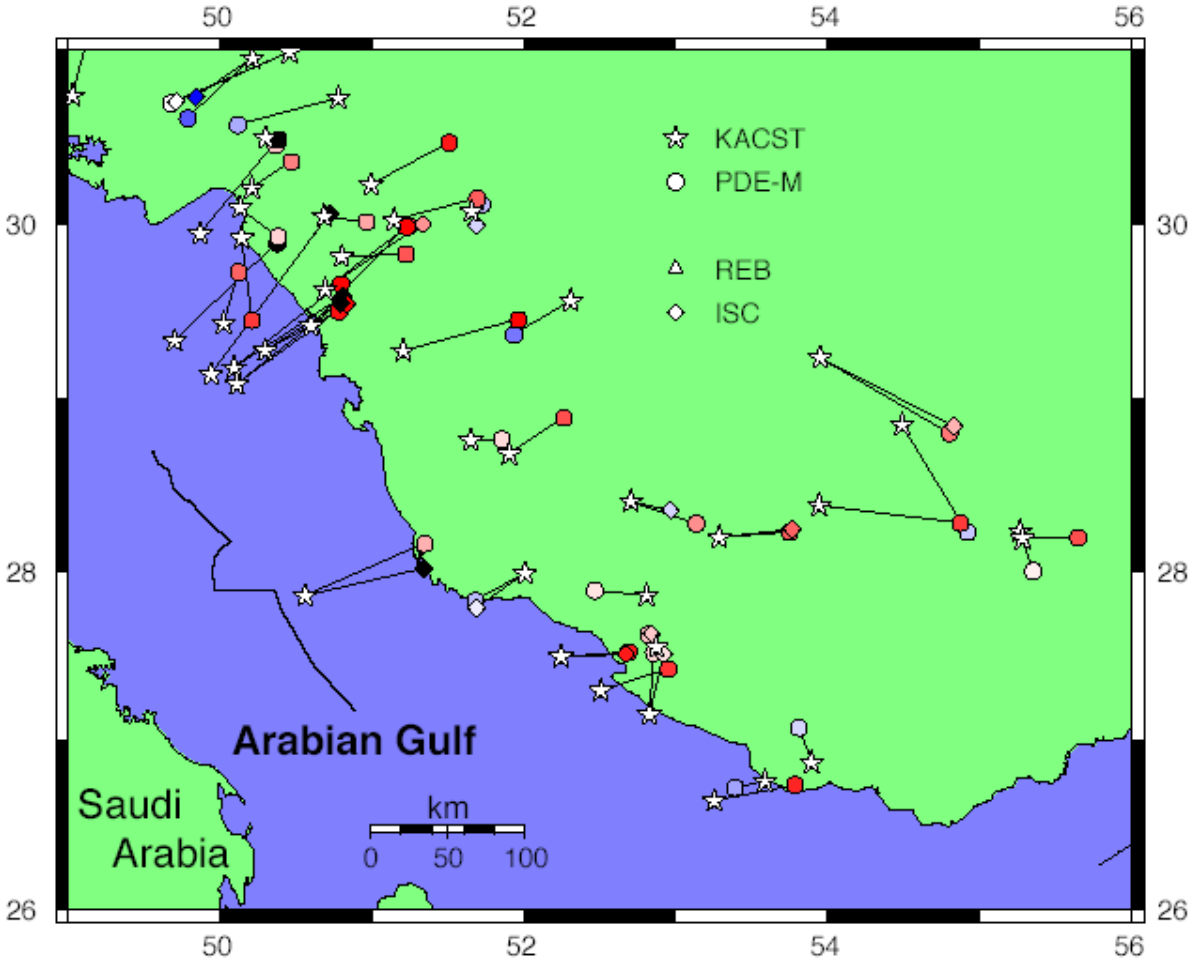

Figure 13. Comparison of SANDSN (stars) and global network locations (other symbols) for the Zagros Mountains region. The color of the symbols for global network locations are scaled by the origin time difference.

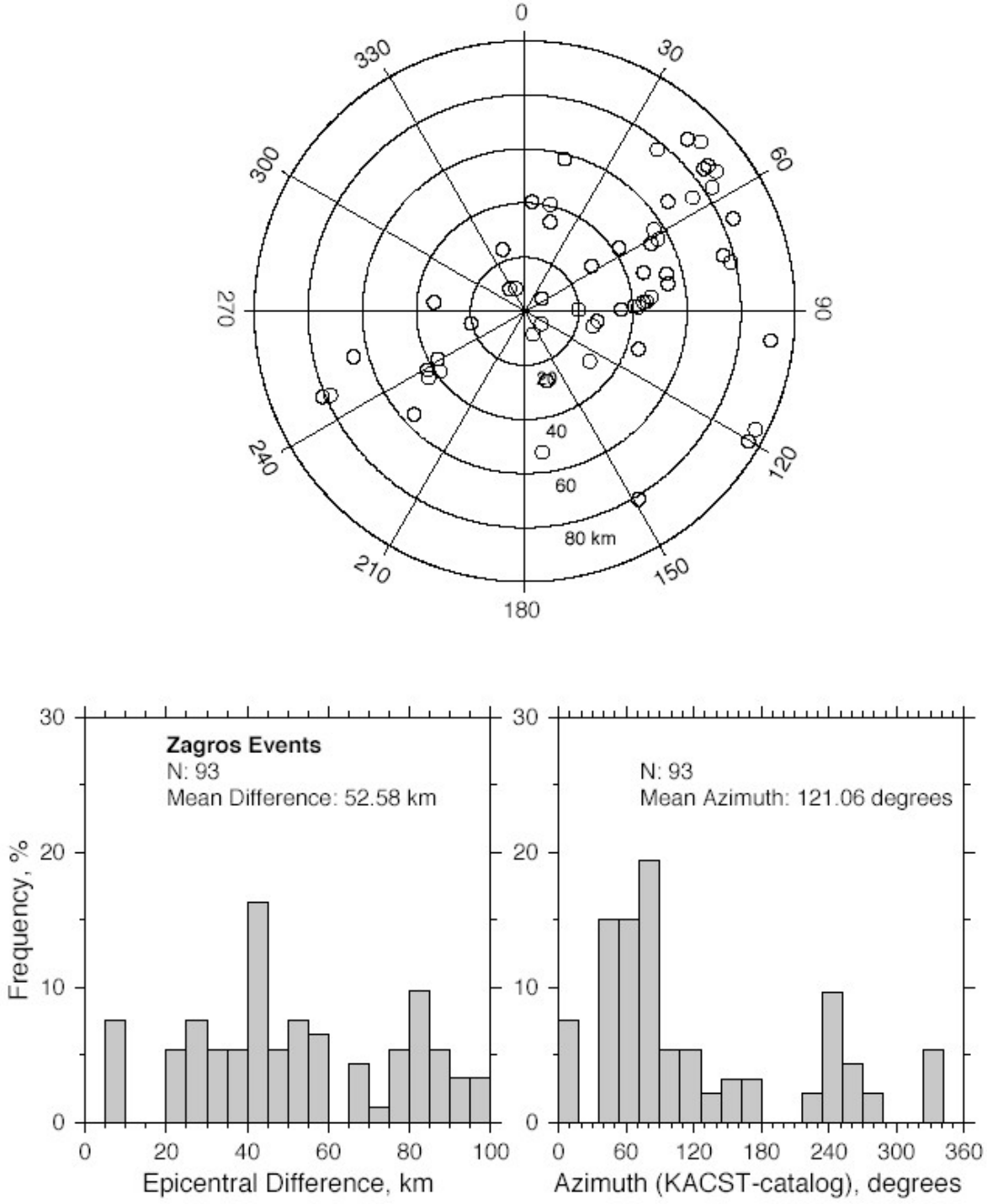

Figure 14. Statistical characterization of location differences between SANDNSN and global network locations for the Zagros Mountains region: (top) azimuth and distance; (left) epicentral difference; (right) directional bias in locations.

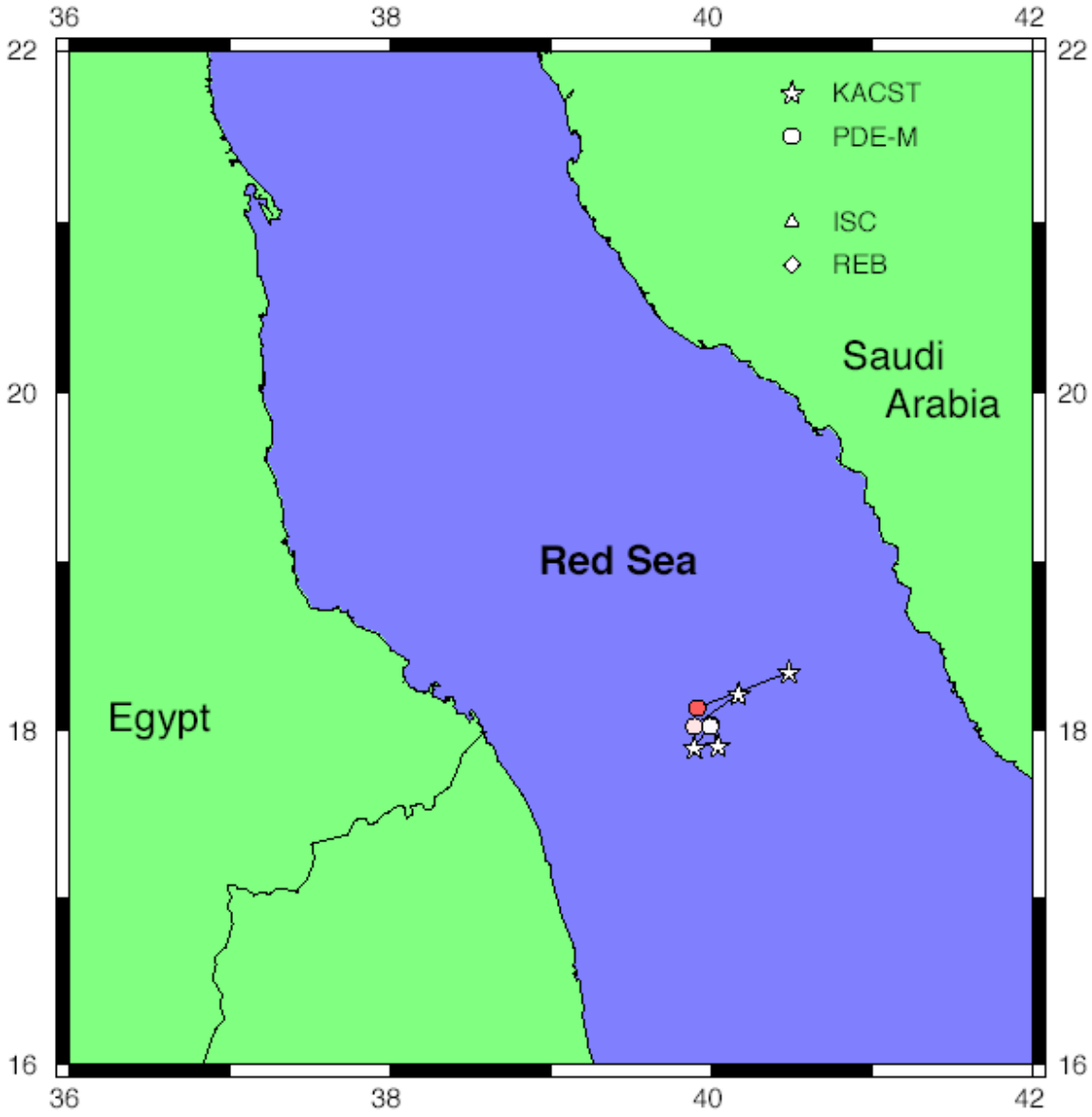

Figure 15. Comparison of SANDSN (stars) and global network locations (other symbols) for the Red Sea region. The color of the symbols for global network locations are scaled by the origin time difference.

Dead Sea Explosions

The best data for calibrating travel times to improve earthquake location are well-coupled controlled source explosions. These experiments use buried explosive sources with well known location and origin time to generate seismic waves that can be observed at large ranges. In November 1999, two such explosions were conducted in the Dead Sea (*Gitterman and Shapira*, 2002). These explosions were well-recorded to about 500 km distance by the SANDSN stations in the Gulf of Aqabah and northwestern Saudi Arabia. Figure 16 shows a map of the explosion locations and the recording stations in Saudi Arabia, including stations from the King Saud University Seismic Network. Details of the explosion location, origin time and yield are given in Table 2. Both shots were detonated in the water at 70-73 m depth.

A smaller shot (500 kg) was conducted on November 8, 1999, but we did not analyze the data because the signal-to-noise was poor on the Saudi networks. The Middle East has dense coverage of seismic stations due to the relatively high population density and earthquake hazard along the Gulf of Aqabah-Dead Sea Rift.

The SANDSN system detected and located the events, however their locations are quite far from the know n (ground truth) locations, indicated in Figure 16 and Table 3.

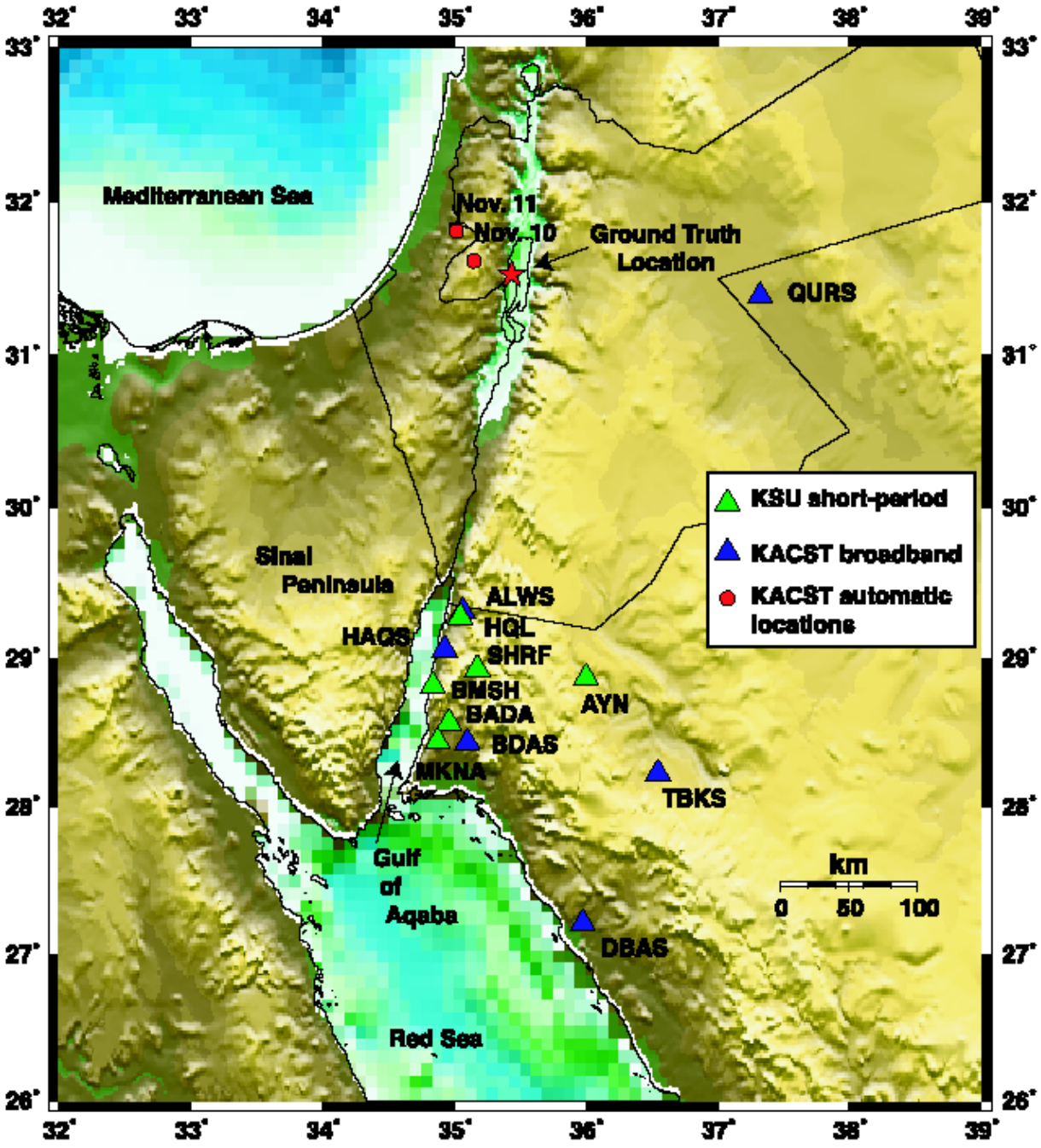

Figure 16. November 1999 Dead Sea explosions and recording stations (triangles) in Saudi Arabia. The SANDSN locations (circles) are quuite far from the groun truth locations (stars).

Table 2. Ground Truth Locations (*Gitterman and Shapira*, 2002)

LATITUDE	LONGITUDE	DATE	TIME (GMT)	YIELD (KG TNT)
31.5338	35.4400	Nov. 10, 1999	13:59:52.210	2060
31.5336	35.4413	Nov. 11, 1999	15:00:00.795	5000

Table 3. Automatic Locations of Dead Sea Shots by Saudi National Seismic Network

LATITUDE	LONGITUDE	DATE	TIME (GMT)	MISLOCATION (KM)
31.6214	35.1506	Nov. 10, 1999	13:59:58.807	29.1
31.8143	35.0178	Nov. 11, 1999	14:59:58.572	50.7

Generally, explosions are detected and located by regional networks and range in magnitude up to m_b 3.5. Events of this type are of interest to regional network operators and nuclear monitoring researchers for several reasons. First, they pose a significant detection, association and location load to nearby stations and networks. Second, chemical explosions can have similar characteristics to underground nuclear explosions (such as the absence of low-frequency S-wave energy) and can fail event screening and discrimination tests. This can place a significant processing load on nuclear treaty monitoring systems. Finally, mining events can be useful for monitoring because they can provide valuable calibration data for event location and characterization. If one knows the location and origin time of mining explosions, then the recordings can be used to calibrate path-dependent travel times.

The observed waveforms from the largest event (November 11, 1999) are plotted in Figure 17. These waveforms show clear Pn, Pg and Sg arrivals, marked by the vertical lines on the seismograms The travel times of Pn, Pg and Sg were used to develop a velocity model of the

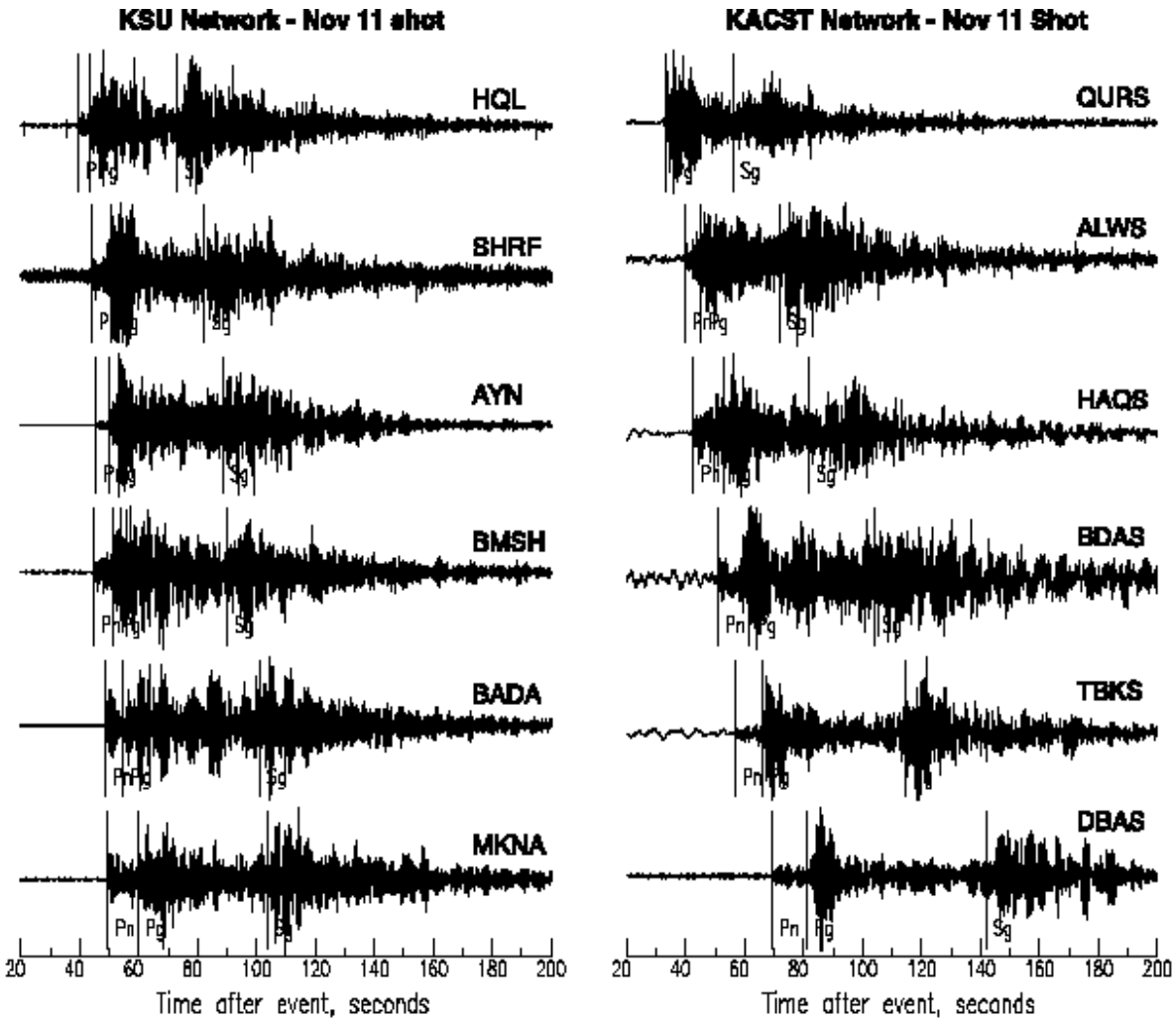

Figure 17. Waveforms from the largest Dead Sea explosion (November 11, 1999).

crust and uppermost mantle for the Dead Sea Rift region. The crustal S-wave, Sg, is observed on all seismograms, despite the source being an explosion in water. Strong Sg energy may be generated by Rg-to-Sg conversions near the source (*Myers et al*., 1999). Sn was not clearly observed for these data, including the horizontal components of the KACST network stations. Sn is not expected to propagate efficiently along the paths studied. Previous studies report inefficient Sn propagation in the Dead Sea Rift (*Kadinsky-Cade et al*., 1981; *Rodgers et al*., 1999). Inefficient propagation of short-period mantle S-waves probably results from attenuation and is related to low seismic velocities directly below the Moho.

We regressed the travel times of each phase versus distance. Data from both shots were included in this analysis. The data and regression models and errors are shown in Figure 18. The fact that both explosions have very similar travel times to each station suggests that there are not timing errors at the stations between the two shots. The slopes of the Pg and Sg travel times versus distance should reflect the average P- and S-wave velocities of the crust, while the Pn travel time slope should indicate the average sub-Moho P-wave velocity. However, caution must be exercised because two-dimensional structure along the path could bias the results. In fact analysis of seismic refraction data sampling the Sinai Peninsula margin of the Gulf of Aqabah indicates that crust thins from about 30 km north of the Gulf to 20 km at the southern-most tip of the Peninsula (*Ginzburg et al.,* 1979).

The slopes of Pg and Sg imply low average crustal velocities (6.28 km/s and 3.43 km/s for P- and S-waves, respectively), consistent with felsic upper crustal compositions of typical continental sections (*Christensen and Mooney*, 1995; *Rudnick and Fountain*, 1995). The average Pn velocity of 7.75 km/s is lower than the global average (8.09 km/s; *Christensen and Mooney,* 1995) but consistent with the seismic refraction study of *Ginzburg et al*., (1979) and the Pn

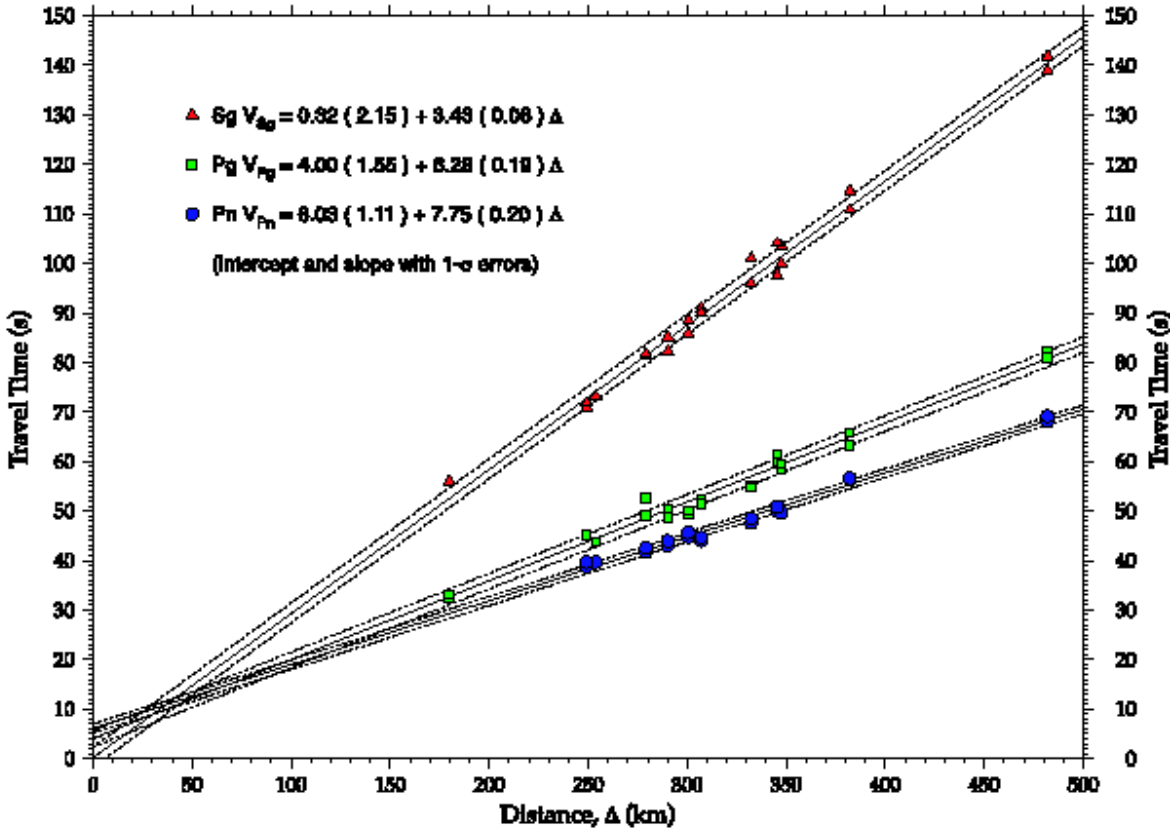

Figure 18. Travel times versus distance for regional phases Pn (blue circles), Pg ((green squares) and Sg (red triangles). The arrival times are fit to linear regression models and the resulting models are plotted and parameters are given in the figure.

tomography study of *Hearn and Ni* (1994). The absence of short-period Sn propagation in the region and low Pn velocities may be consistent with the presence of partial melt in the shallow mantle. The regression fits indicate that the Pn intercept time is quite small (6.03 ± 1.11 s). This would imply a thin crust (~12 km) and a short Pn-Pg crossover distance (< 100 km). However, Pg appears to be the first arrival at station QURS (Figure 17), implying a thicker crust. A crustal thickness of about 30 km for the Dead Sea region is reported from studies of seismic refraction data (*Ginzburg et al*., 1979) and teleseismic receiver functions (*Sandvol, et al*., 1998). The inclusion of data from station QURS may be problematic if the structure to the east of the Dead Sea is dramatically different from that to the south.

The sensitivity of travel times to one-dimensional (1D) average velocity structure is certainly non-unique and our goal is to find a range of models that fit the data reasonably well and are consistent with what is already known about the region. By using a grid search technique we avoid problems associated with linearizing the dependence of the data on model parameters, as is required by linear inversion methods.

We performed the grid search using travel time data sets: (a) Pn and Pg; and (b) Pn, Pg and Sg. We considered two data sets for two reasons. Firstly, the onset times of Sg are more difficult to pick, so it may not be prudent to include the Sg picks in the estimation of structure. Secondly, we are not directly solving for the shear wave velocities, but rather scaling shear velocities to compressional velocities with an assumed Poisson's Ratio, so the influence of Sg travel times may bias the model. The optimal model should reduce the scatter in the data (i.e. minimize the rms) and result in zero-mean residuals. We chose models that resulted in absolute mean residuals less than 0.5 seconds and minimum rms. The threshold on the absolute mean residual was chosen to be a conservative estimate on the picking error. From the 800 models considered we chose the 20 best fitting models according to the criteria described above. The 20 best-fitting models

for both data sets are shown in Figure 19. Both data sets infer similar velocity models, however the models inferred from Pn and Pg data are less scattered. Crustal thicknesses range between 24 and 30 km. The upper crustal velocities are poorly resolved by both data sets. Velocities of the lower crust are 6.0-6.2 km/s.

The absolute mean residual is plotted versus the rms residual for both data sets in Figure 20. This figure illustrates how each model performs toward the goal minimizing the absolute mean residual and residual scatter. Figure 21 shows the fit of the 20 best-fitting models to the Pn, Pg and Sg travel times for the case when all three phases are fit simultaneously. One can see that the data are only weakly sensitive to changes in the crustal velocities. Comparison with the error bars shows that the theoretical travel time curves pass within two standard deviation of observed travel times. Thus, based on travel times alone, we cannot reject any of these models at the 2-σ level.

In order to select a single velocity model to be representative of the paths sampled, we made use of the results of a seismic refraction (*Ginzburg et al*., 1979) and a recent composite model of crustal thickness (*Seber et al*., 1997). Our grid search results with the thicker crusts (28-30 km) are consistent with these earlier studies. The preferred model has a crustal thickness of 28 km and is compiled in Table 4.

Table 4. Preferred Velocity Model for the Gulf of Aqabah/Dead Sea Region

DEPTH (KM)	THICKNESS(KM)	V_P (KM/S)	V_S (KM/S)
0	2	4.50	2.60
2	5	5.50	3.18
7	10	6.10	3.52
17	11	6.20	3.60
28	∞	7.80	4.37

V_P and V_S are the P- and S-wave velocities, respectively.

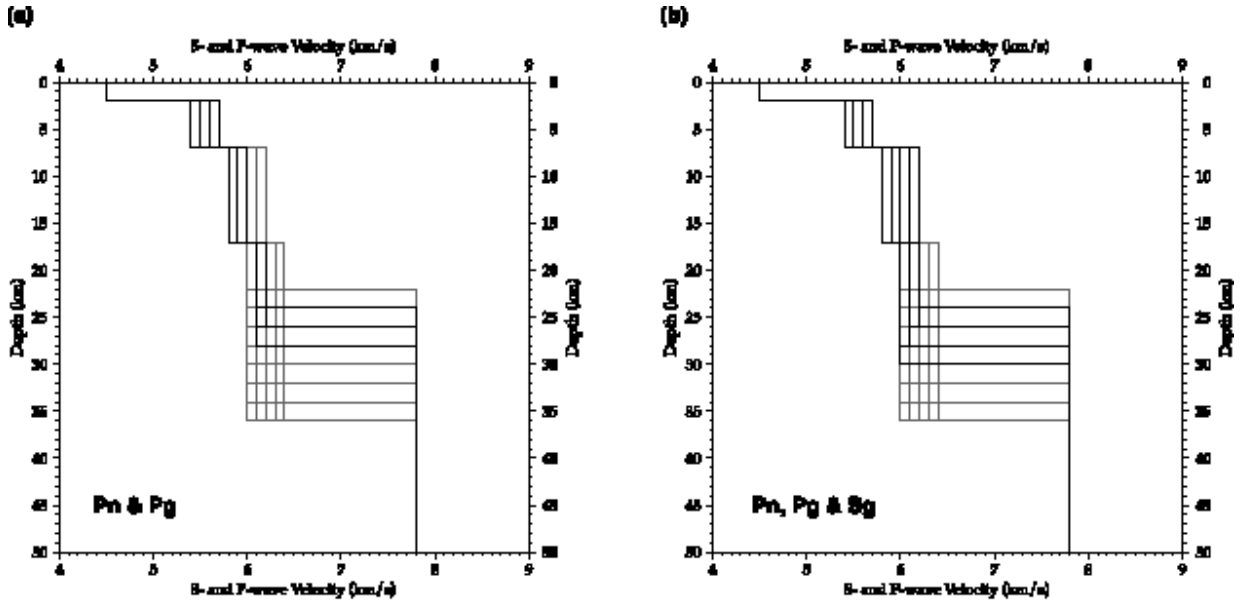

Figure 19. P-wave velocity models investigated in the grid search (thin gray lines). The 20 best-fitting models are also shown (thicker black lines) for two travel time data sets (a) Pn and Pg; and (b) Pn, Pg and Sg.

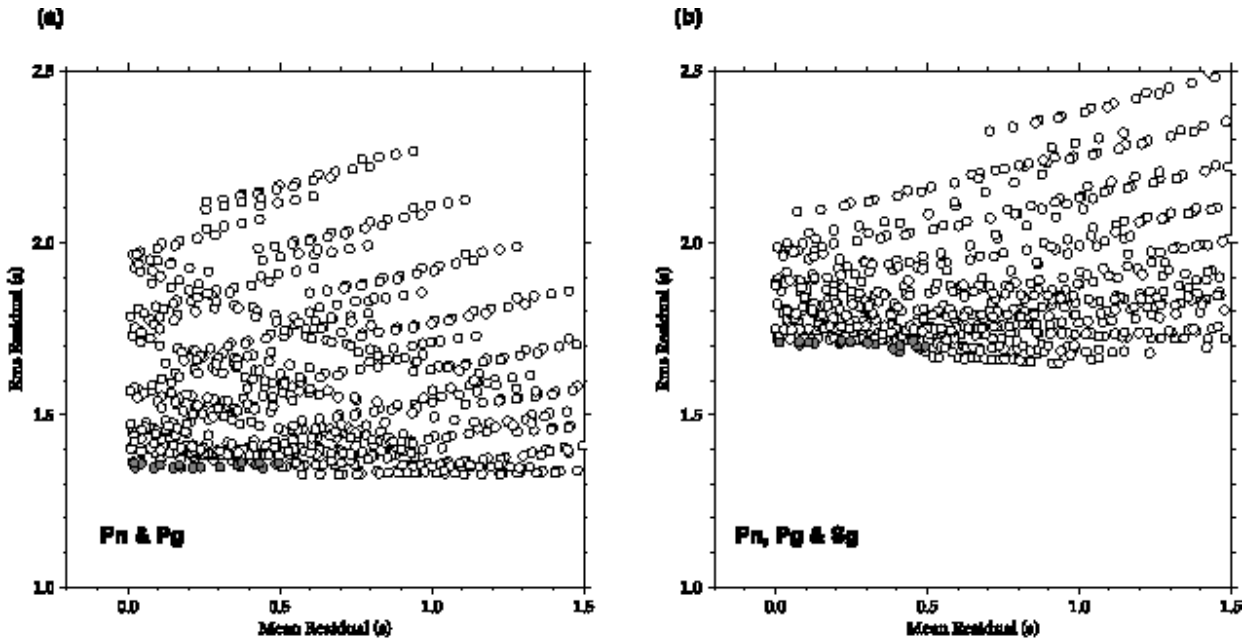

Figure 20. Plot of absolute mean and root-mean square (rms) residual for each model plotted in Figure 4 (open circles). The grey circles indicate the best-fitting models chosen to have an absolute mean less than 0.5 seconds and a minimum rms. Cases for two data sets are shown: (a) Pn and Pg; and (b) Pn, Pg and Sg.

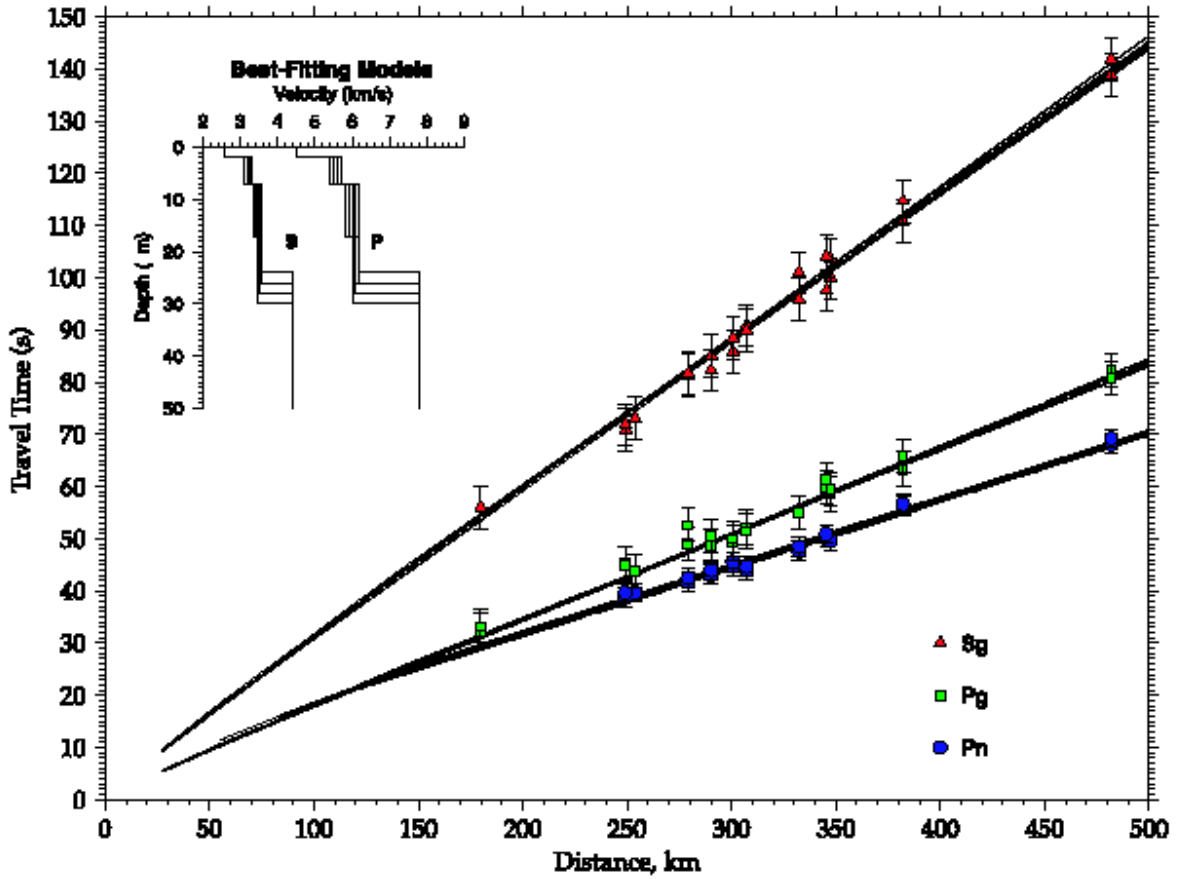

Figure 21. Observed Pn, Pg and Sg travel times (symbols), 2-s errors and the predictions of the best 20 models when all three phases are considered together (lines). The inset figure shows the best-fitting models.

6. DISCUSSION & INTERPRETATION

6.1 Arabian Platform and Shield Models from Surface Wave Dispersion and Waveform Modeling

Earlier work with waveform data from the 1995-1997 Saudi Arabian Broadband Deployment by the University of California, San Diego (UCSD) and King Saud University resulted in models for the Arabian Platform and Arabian Shield *(Rodgers et al.*, 1999). In that studied Love and Rayleigh wave group velocities were modeled to estimate average one-dimensional seismic velocity models of the two main geologic/tectonic provinces of Saudi Arabia. A grid search was used to quickly find a range of models that satisfactorily fit the dispersion data, then that range of models was explored to fit the three-component broadband (10-100 seconds) waveforms. The resulting models revealed significant differences between the lithospheric structure of the two regions. The resulting models are plotted in Figure 4 along with the *iasp91* model (*Kennett and Engdahl*, 1991) and our Gulf of Aqabah/Dead Sea model (*Rodgers et al.*, 2001). The Arabian Shield and Platform models are compiled in Tables 5 and 6, respectively.

Table 5. Preferred Velocity Model for the Arabian Shield Region

DEPTH (KM)	THICKNESS(KM)	V_P (KM/S)	V_S (KM/S)
0	1	4.0	2.31
1	15	6.20	3.58
16	20	6.80	3.93
36	∞	7.90	4.30

V_P and V_S are the P- and S-wave velocities, respectively.

Table 6. Preferred Velocity Model for the Arabian Platform Region

DEPTH (KM)	THICKNESS(KM)	V_P (KM/S)	V_S (KM/S)
0	4	4.00	2.31
4	16	6.20	3.64
20	20	6.4	3.70
40	∞	8.10	4.55

V_P and V_S are the P- and S-wave velocities, respectively.

6.2 Surface Wave Group Velocity Analysis

To check the validity of our model for the Arabian Platform, we measured Rayleigh and Love wave group velocities for a number of regional events from the Zagros Mountains and Turkish-Iranian Plateau. Paths from these events to the SANDSN stations sample the Arabian Platform. The events considered and the resulting dispersion curves are shown in Figure 22. We also show the predictions for our Arabian Platform velocity model (*Rodgers et al.,* 1999). This model was derived from paths sampling the Arabian Platform to stations on the eastern most Arabian Shield, thus they sample nearly the entire sedimentary structure of the Arabian Platform (Figure 2). We computed an average sediment thickness for these paths, however the new paths considered in Figure 22 sample more diverse paths.

Working with Dr. Michael Pasyanos (LLNL) and Ms. Maggie Benoit (Pennsylvania State University), we constructed a tomographic model of surface wave group velocities for the Arabian Peninsula and Africa Rift regions. Figure 23 shows the resulting tomographic image of 20 second Rayleigh wave group velocities. The image shows slower than average velocities for the Arabian Platform and Rub Al-Khali, probably due to low-velocity sediment cover. The Red Sea is faster than average due to thinner crust. The 20 second group velocities gradually

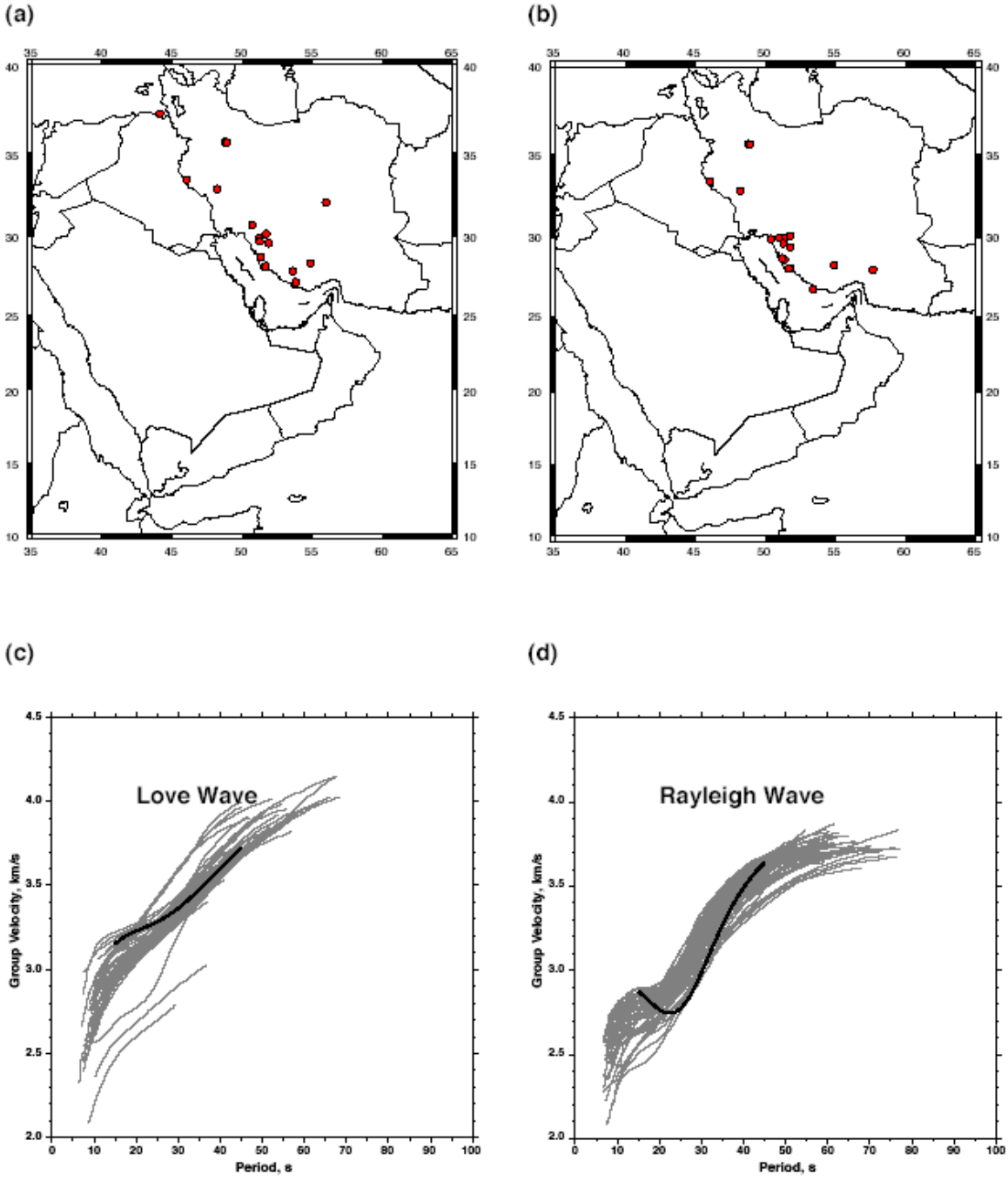

Figure 22. Surface wave group velocity dispersion analysis. Events considered for (a) Love and (b) Rayleigh waves. Group velocity dispersion curves for (c) Love and (d) Rayleigh waves (gray). The thick black lines in (c) and (d) show the predictions from the Arabian Platform model (Rodgers et al., 1999).

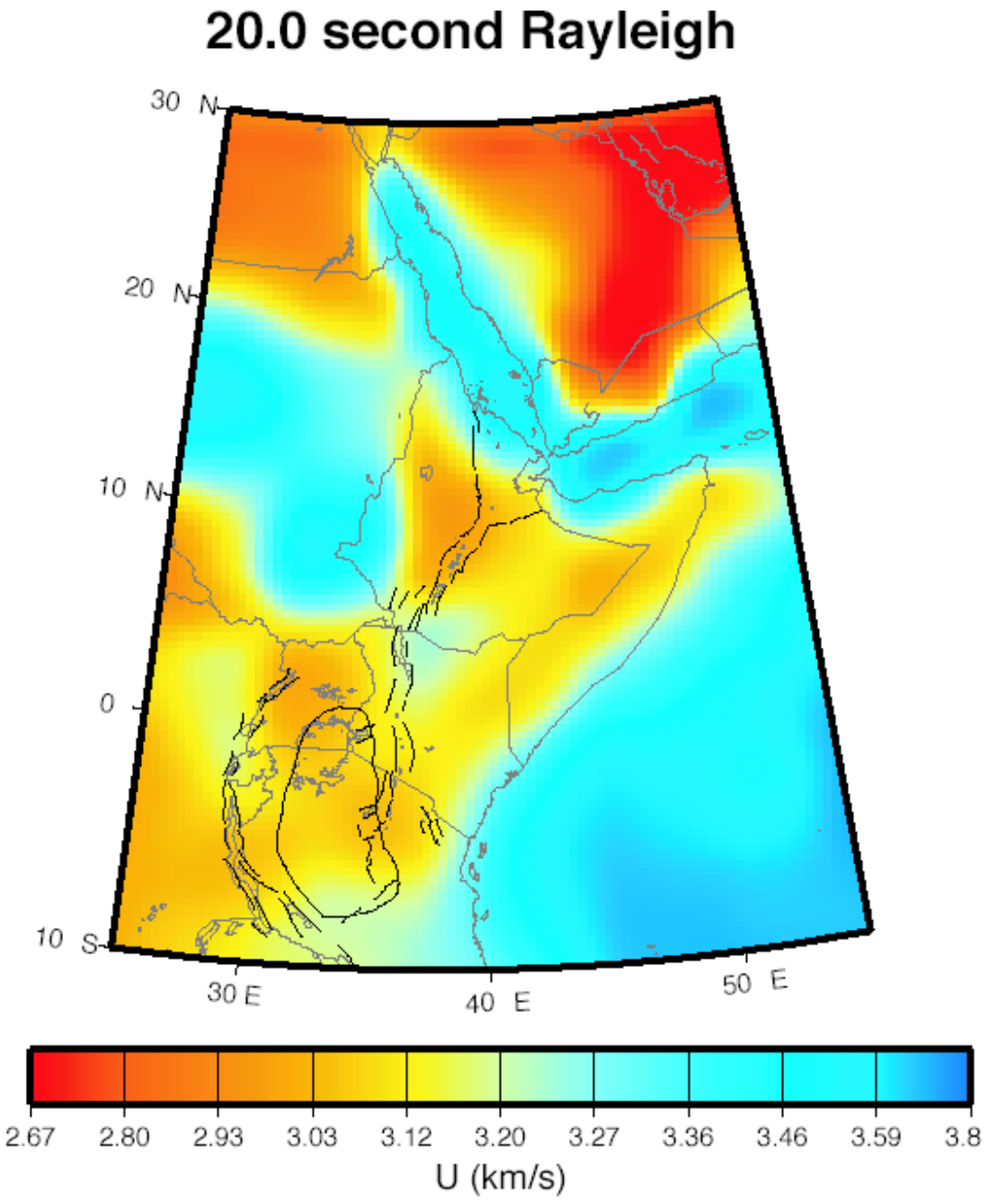

Figure 23. Rayleigh wave group velocities at 20 seconds for the Arabian Peninsula, African Rift and surrounding regions.

increase from the Eastern Province to the Hejaz and Red Sea. The inclusion of additional surface wave dispersion data could help resolve three-dimensional structure of Saudi Arabia.

6.3 Evaluation of SANDSN Timing with P-wave Arrival Times

In order to check the timing at the SANDSN stations and to measured relative P-wave arrival times with an accurate cross-correlation method (*VanDeCarr and Crosson*, 1990). This method finds the optimal relative timing of vertical component P-waves at a set of stations. The travel time residuals are then computed relative to a layered earth model, such as *iasp91* (*Kennett and Engdahl*, 1991). This method was used by *Benoit et al.* (2002) to image P-wave velocity anomalies beneath the Arabian Shield. Residual uncertainties are typically 0.05-0.1 seconds. We used the method to check the relative timing of the SANDSN stations to identify possible timing errors at the stations. Modern seismic recording systems use GPS timing at the site and are less likely to have problems compared with older systems. The pattern of travel time residuals is shown in Figure 24 for four events with different azimuths. The residuals are quite small ranging about 1.5 seconds. This range is consistent with that found by *Benoit et al*. (2002) and is likely related to upper mantle P-wave velocity structure and not due to timing problems at the stations.

6.4 Evaluation of Arabian Velocity Models with SANDSN Travel Times

The seismic velocity models described above are emblematic of the variability in thermal and compositional structure related to complex tectonic processes at work in the Arabian Peninsula. Figure 25 shows the predictions of first-arriving P-wave for a surface focus (zero depth) event for the range 0 –20 degrees (0-2222 km). The models predict arrival time differences of as much as several seconds.

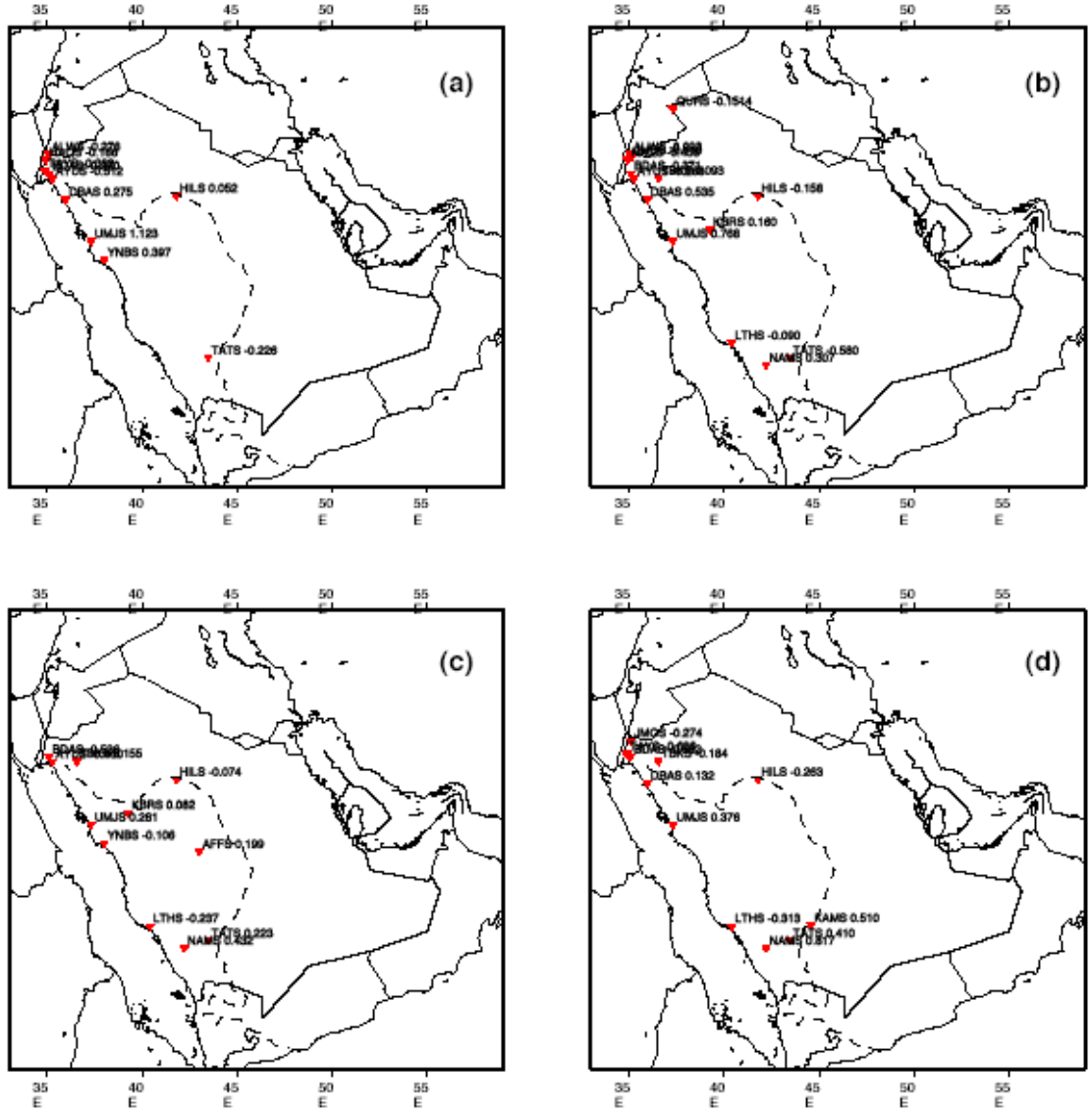

Figure 24. Relative P-wave travel time residuals measured by multi-channel cross-correlation. The travel time residuals are given as text near each recording station for four evnets at approximate azimuths of (a) 63 degrees, (b) 82 degrees, (c) 182 degrees and (d) 256 degrees.

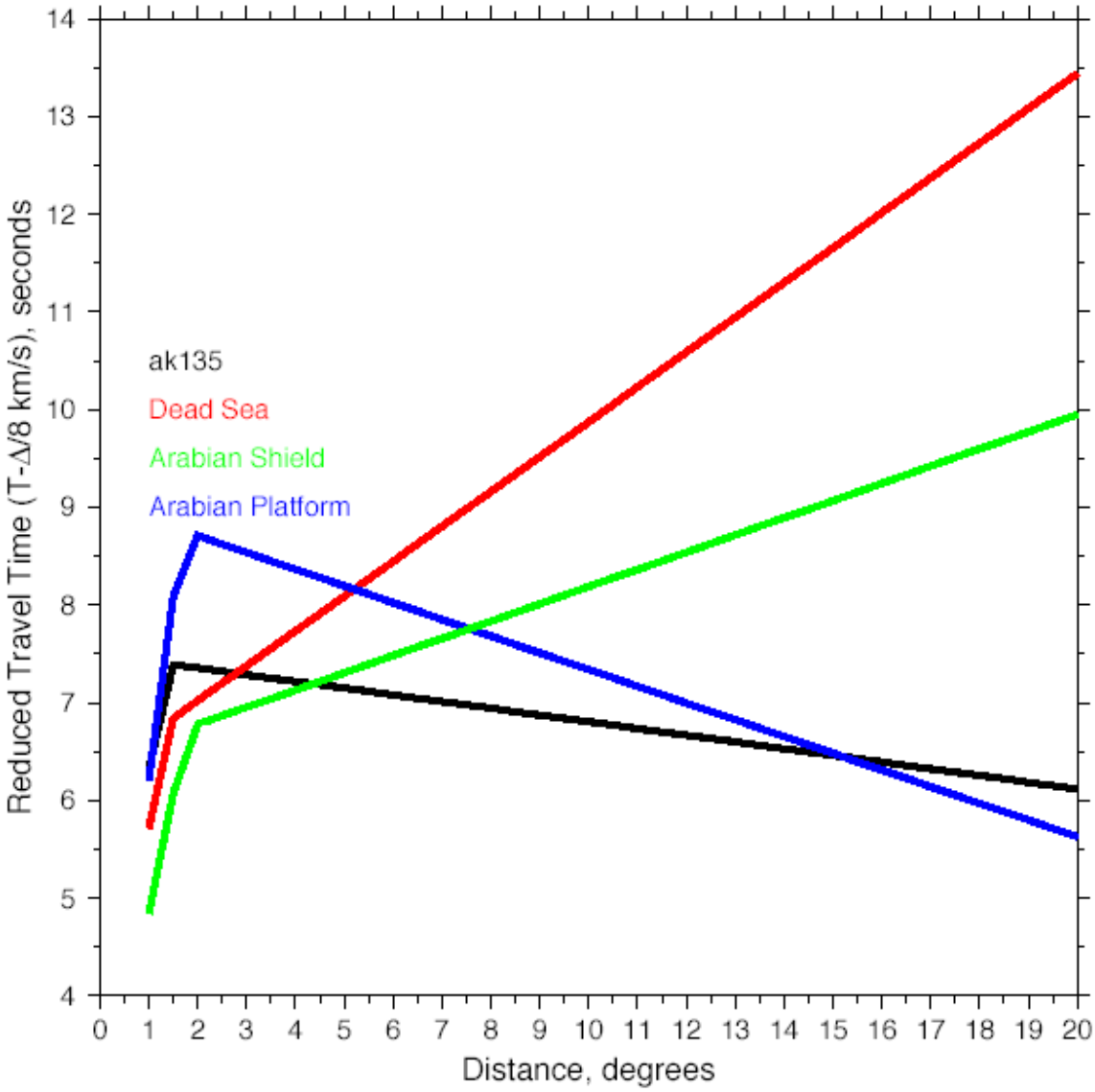

Figure 25. Travel time curves for first-arriving P-wave for a surface focus event for four models: iasp91 (black, Kennet and Engdahl, 1991); the Gulf of Aqaba/Dead Sea (red, Rodgers et al., 2001) the Arabian Platform (blue) and Arabian Shield (green) (Rodgers et al., 1999).

In order to check the validity of travel time predictions from our proposed seismic velocity models, we compared observed travel times for well-located earthquakes. We chose to use waveforms from the 1995-1997 UCSD-KSU Saudi Arabian Broadband Deployment. We did this for two reasons. Firstly, we had limited KACST waveform data to work with. Secondly, we used earthquake locations from the International Seismological Centre (ISC). These locations rely on arrival time reports from all over the world and are delayed by more than two years after an event occurs. We had little or no overlap between our well-located earthquake catalog and KACST data holdings. The available catalog had events in the Zagros Mountains. This provided paths sampling the Arabian Platform. Figure 26 shows the paths and travel times considered. Agreement between the observations and the Arabian Platform model predictions is quite good. The paths sample the faster crust of the Arabian Shield and this may be the reason that the arrivals are on average early compared with the model predictions.

6.5 Focal Mechanisms of Regional Events

A moderate (M~5) earthquake struck the northeastern United Arab Emirates (UAE) on March 11, 2002. The event was large enough to be detected and located by global networks at teleseismic distances. The region is generally believed to be aseismic, however no regional seismic network exists in the UAE to determine earthquake occurrence. This event serves as a test case to illustrate the SANDSN location performance and demonstrate what can be done with broadband waveform data. Local information provided by the United Arab Emirates University (UAEU) Department of Geology, locates this event in or near the town of Masafi, in the Oman Mountains. Figure 27 shows the location of the events from global networks (PDE, REB). Large earthquakes are rare in this part of the world. Most large earthquakes in near eastern Saudi Arabia occur in the Zagros Mountains across the Arabian Gulf in Iran (Figure 27, inset).

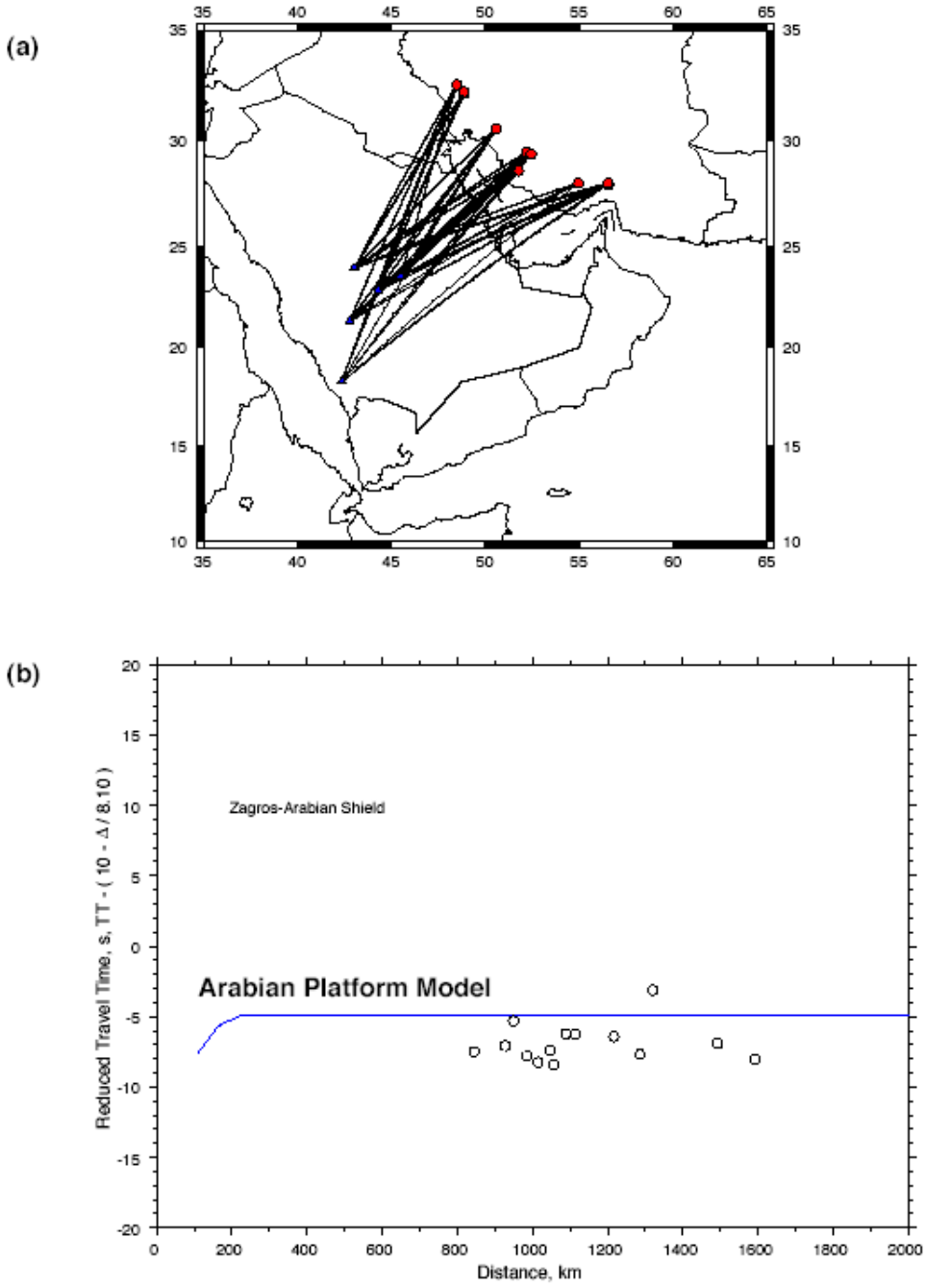

Figure 26. (a) Map of well-located earthquakes in the Zagros Mountains, paths and recording stations of the 1995-1997 UCSD-KSU Saudi Broadband Deployment. (b) Observed travel times (circles) and predictions from the Arabian Platform model (blue line). Both data and predictions are reduced by 8.1 km/s.

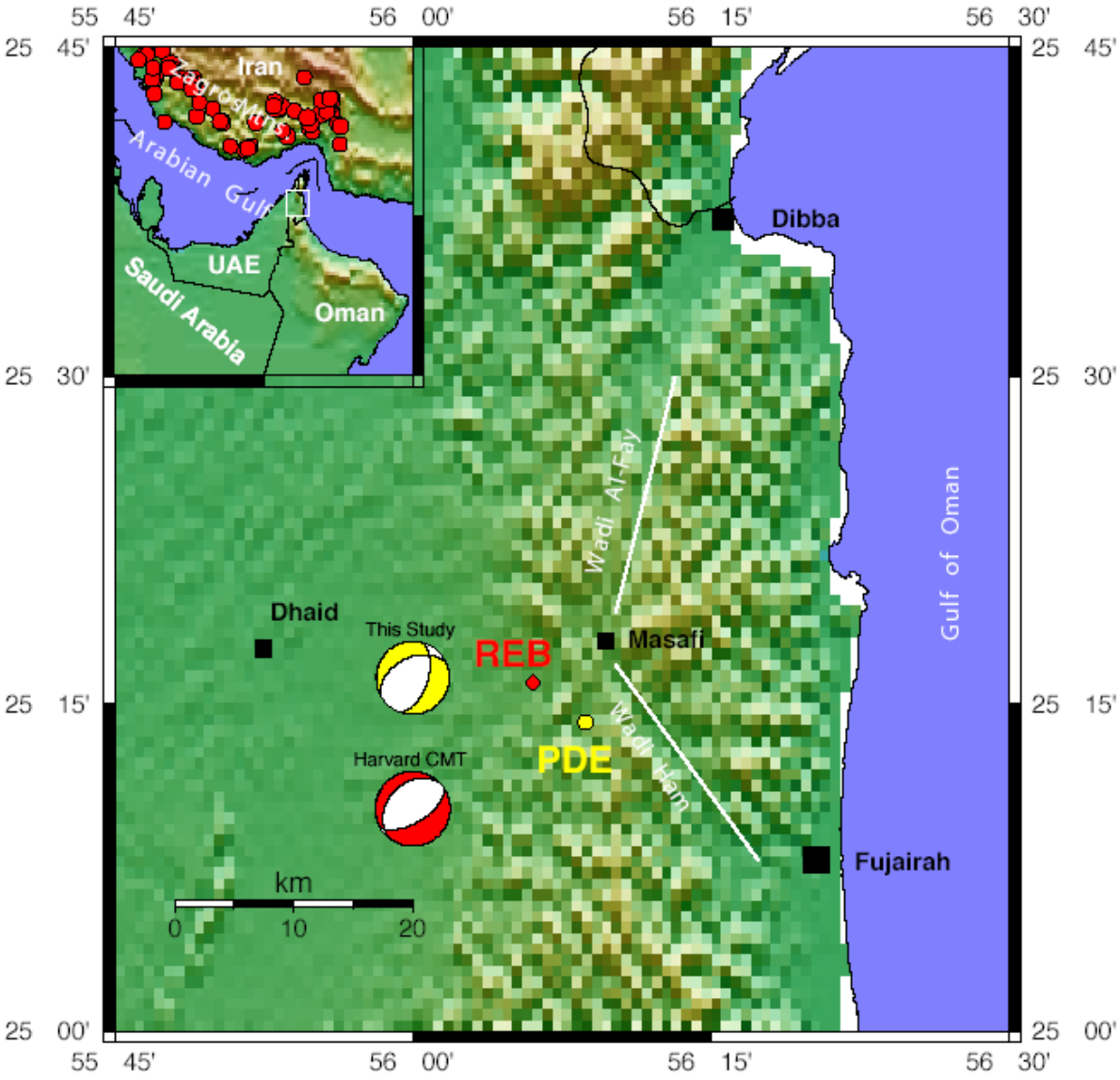

Figure 27. Map of the northeastern United Arab Emirates (UAE) with locations of the March 11, 2002 earthquake, mapped faults and main geographic features. (inset) Map of the UAE and surrounding region with tectonic plate boundaries and large earthquake locations (circles).

Broadband complete regional waveforms were used to estimate a focal mechanism and depth of the event. We combined waveform data from the SANDSN as well as data from the Kuwait Institute for Scientific Research (KISR, station KBD) and the Incorporated Research Institutions for Seismology Global Seismic Network (IRIS-GSN, station ABKT). Figure 28 shows the event location, paths and stations used in the focal mechanism study of this event. We followed the grid search procedure described in *Walter* (1993) to find the best-fitting seismic moment, focal mechanism and depth for each of three stations using appropriate velocity models (Figure 29). Figure 30 shows the misfit (scaled error) and focal mechanism versus depth for the individual stations (HASS, KBD and ABKT) and for the combined three-station fit. The best-fitting solution has a depth of 15 km and moment magnitude of 4.89 and an oblique strike-slip mechanism for the event. The resulting waveform fits for the three-station solution are shown in Figure 31. The focal mechanism is consistent with the broad-scale tectonics of the Arabian-Eurasian collision. To the west to the Musandam Peninsula, Arabia is under thrusting the southern Eurasian margin along the Zagros Thrust. To the east of the Musandam Peninsula, convergence is much slower given the seismicity along the Makran coast. Strike-slip motion probably occurs along reactivated thrust planes associated with obduction of the Semail Ophilite (Oman Mountains).

Finally, we consider the location of the March 11, 2002 Masafi UAE earthquake with the SANDSN data. Figure 32 shows the location of the event from the USGS-PDE and CTBTO-PTS-REB catalogs (same as Figure 27) along with the SANDSN location. Note that the SANDSN location is more than 100 kilometers away from the town of Masafi. While the exact location cannot be known, strong shaking Masafi was felt in Masafi and damage was

Figure 28. Map of the Arabian Peninsula and southern Eurasia showing the event, stations and paths of regional waveforms considered in this study.

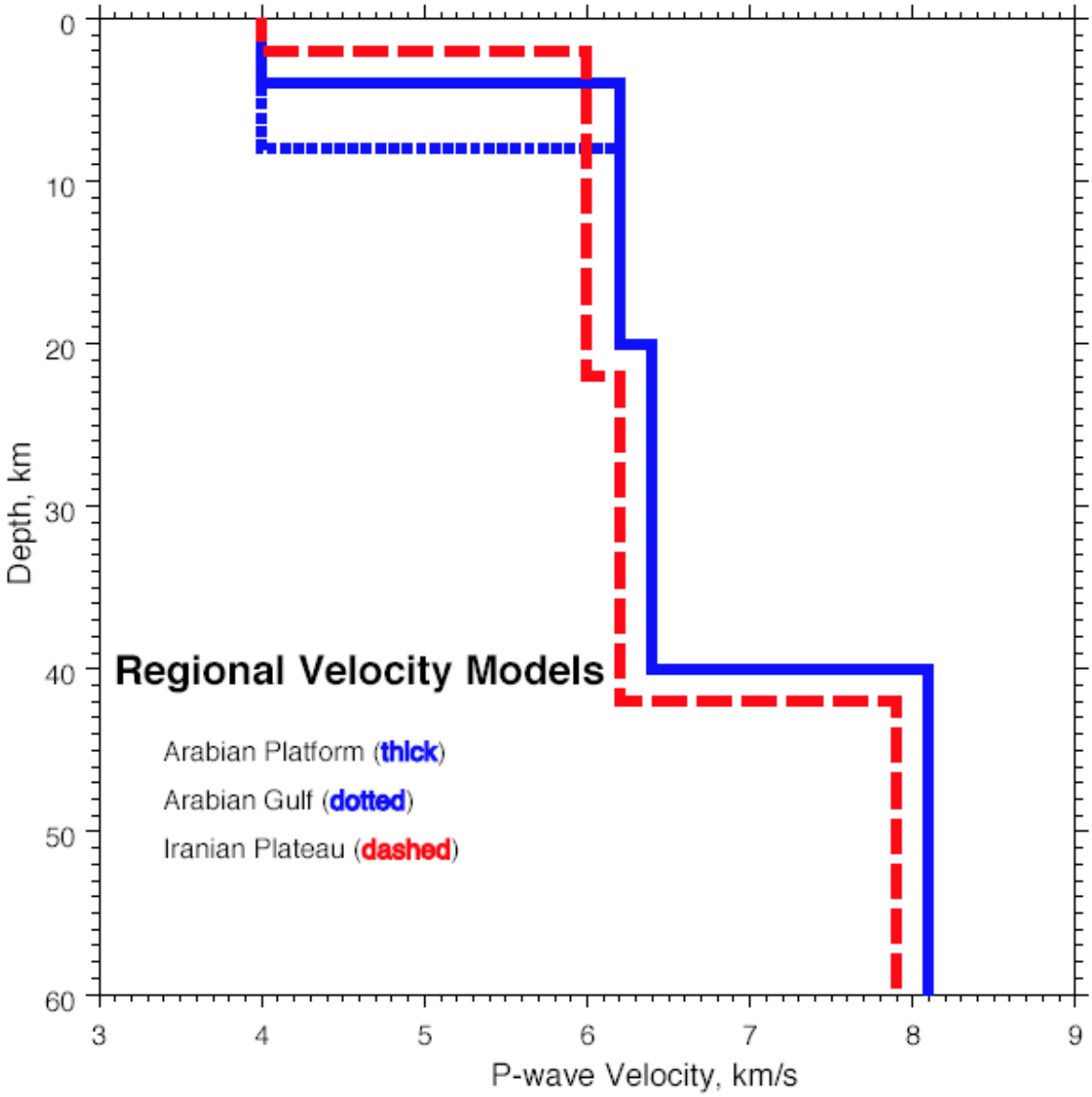

Figure 29. Crustal velocity models used for the synthetic seismogram calculations.

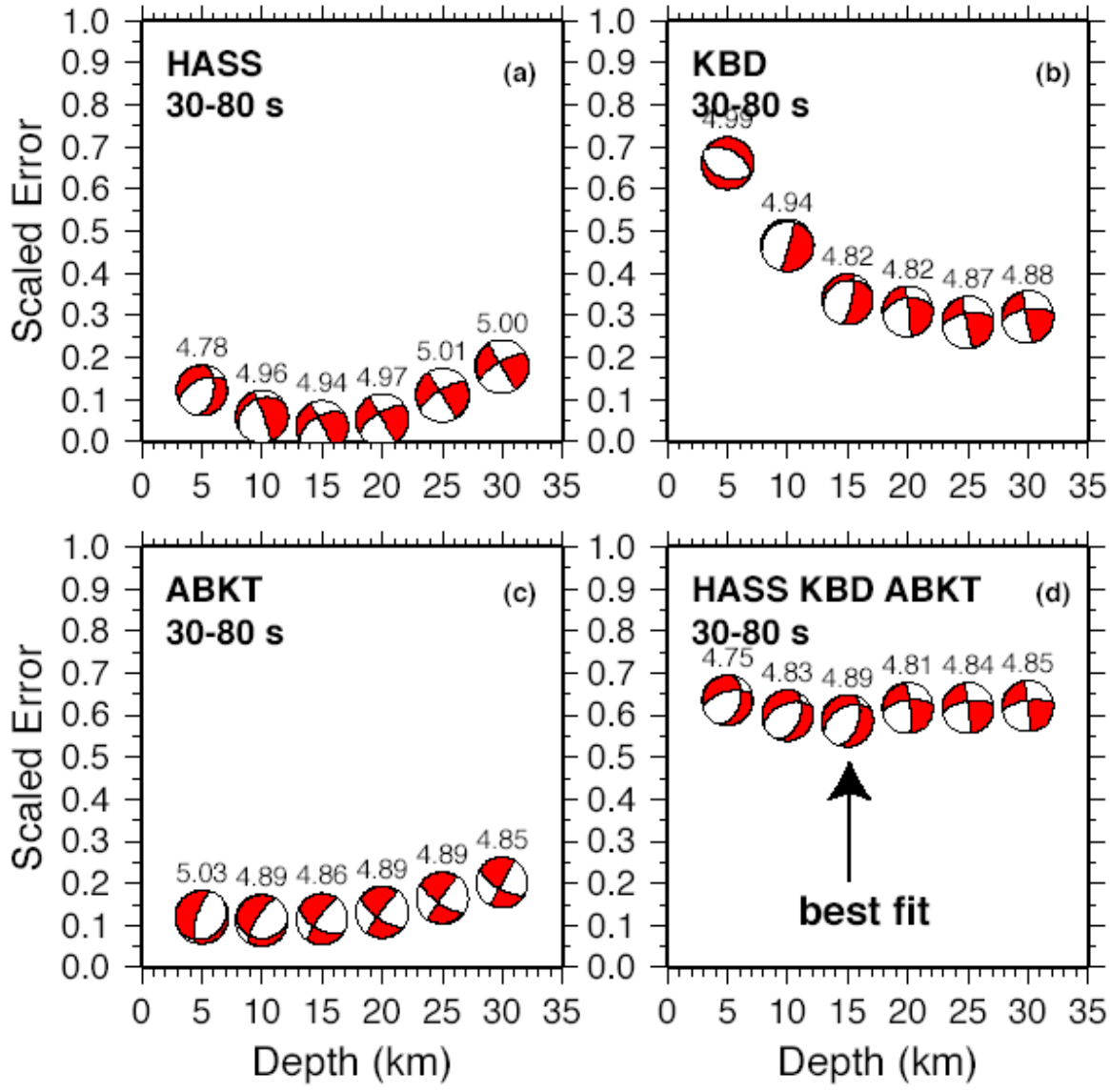

Figure 30. Focal mechanism and scaled error versus depth for the individual three-component station data (a-c, HASS, KBD and ABKT, respectively) and the joint fitting of all three stations (d).

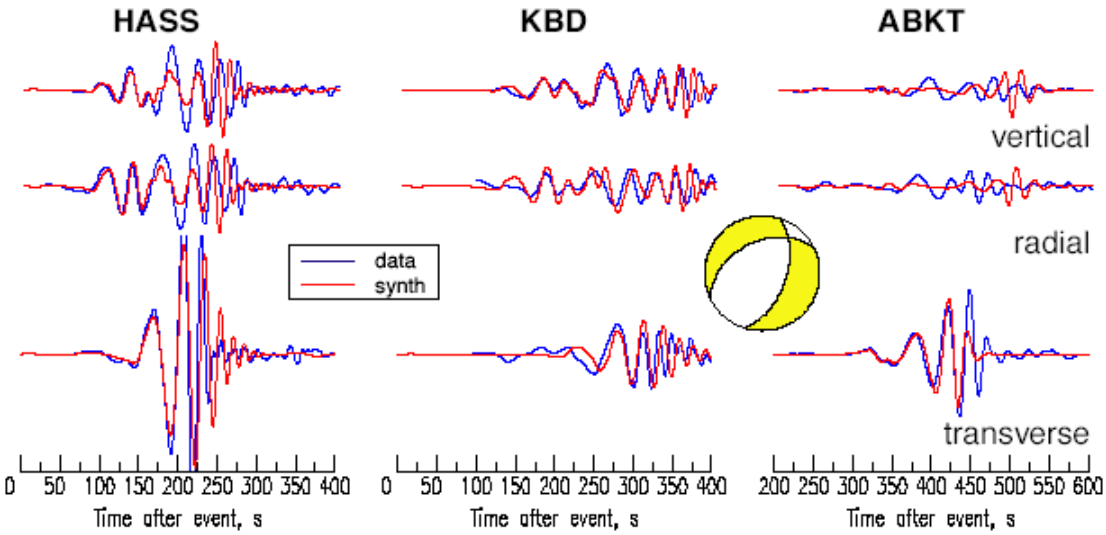

Figure 31. Observed (blue) and synthetic (red) waveforms for the focal mechanism modeling of the March 11, 2002 Masafi, UAE earthquake. The best-fitting focal mechansim is also shown in the figure.

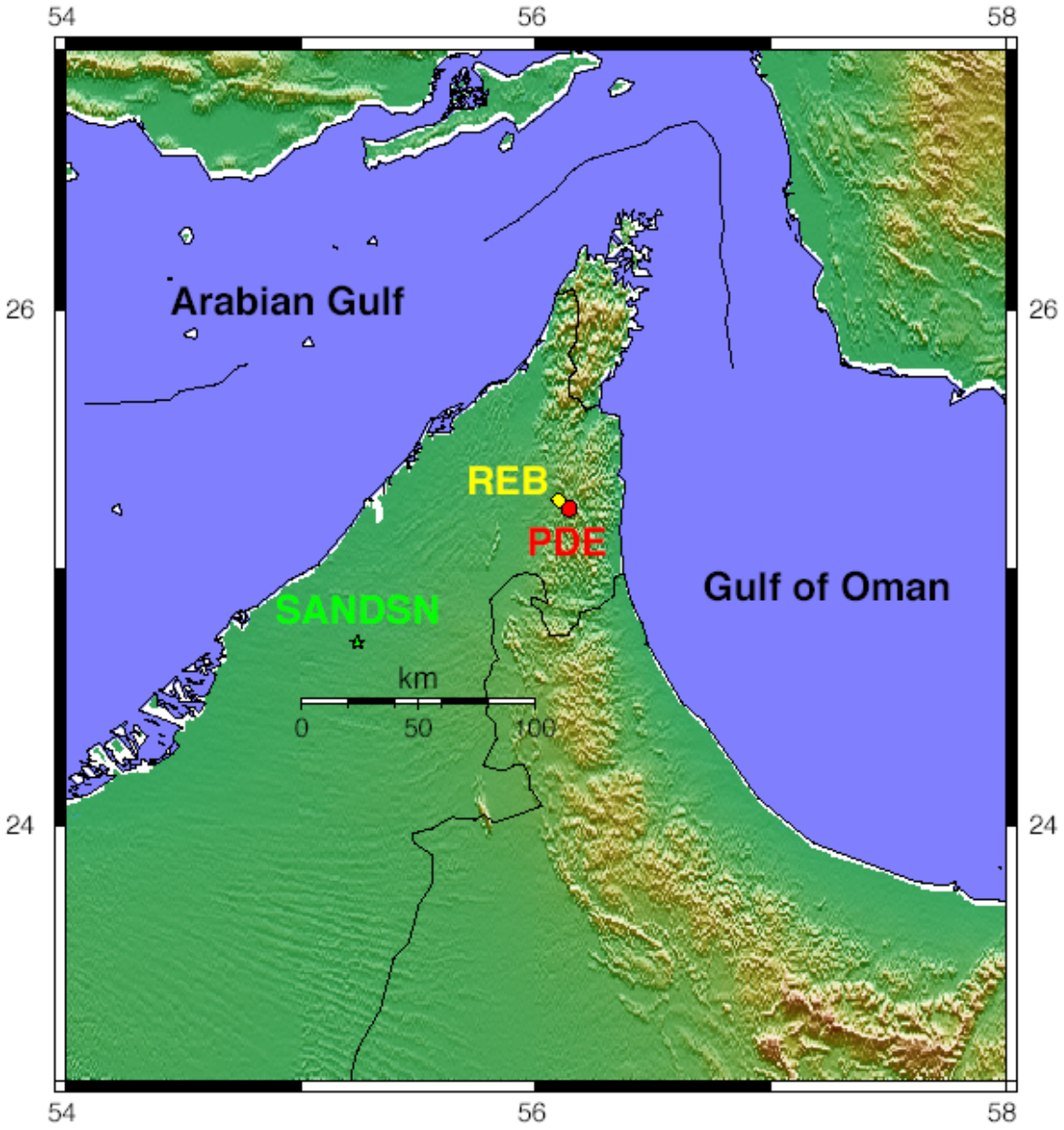

Figure 32. Map of the Musandam Peninsula (United Arab Emirates and Oman) with the estimated locations of the MArch 11, 2002 Masafi earthquake. The location by the SANDSN system (green star) is quite far from the locations by the USGS-PDE (red circle) and CTBTO-PTS-REB (yellow diamond) and the town of Masafi, where the event was strongly felt.

recorded, so the earthquake must have been within 5-10 kilometers of the epicenter. The large mislocation error by the SANDSN system is again probably due to the inadequate velocity model.

Figure 33 shows the reduced travel times and the predictions of the iasp91 model (*Kennett and Engdahl,* 1991) and the Arabian Platform model. The Arabian Platform model provides a good prediction of the travel times to SANDSN stations. Sites in the Asir region show negative residuals, probably due to faster crustal velocities than the Arabian Platform. Sites in Kuwait have positive residuals, probably due to slower than average crustal and sediment velocities.

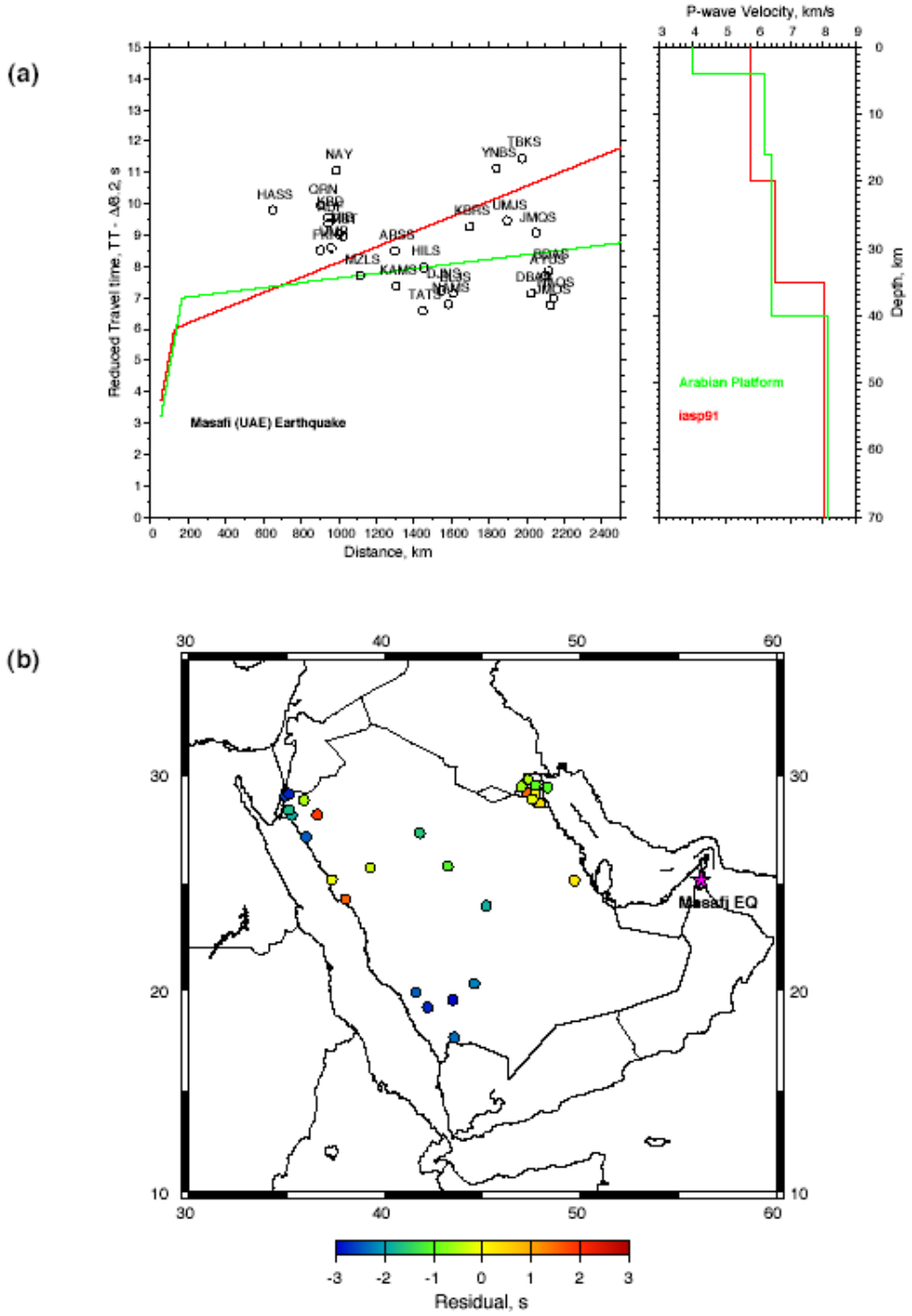

Figure 33. (a) P-wave travel times for the March 11, 2002 Masafi earthquake to stations in SANDSN and Kuwait networks. Also shown are predictions from the iasp91 and Arabian Platform models. (b) Map of travel time residuals relative to the average model (similar to the Arabian Platform model). Note the pattern of residuals with the Kuwait stations showing positive (slow) residuals and the Asir stations showing negative (fast) residuals.

7. CONCLUSIONS & RECOMMENDATIONS

1) The Saudi Arabian National Digital Seismic Network (SANDSN) is an excellent, state-of-the-art seismic network. The sites are quiet and noise surveys at a few stations indicate that seismic noise levels at SANDSN stations are quite low for frequencies between 0.1 and 1.0 Hz, however cultural noise appears to affect some stations at frequencies above 1.0 Hz. Broadband waveform data is generally comparable with data from the Global Seismic Network operated by the Incorporated Research Institutions for Seismology (IRIS-GSN).

2) We found no evidence of timing problems with the data. The sample rate (currently set at 100 samples/second) can be lowered to 50 samples/second without any loss of information. The current high sample rate has several unwanted consequences. Firstly, the high sample rates taxes network communications and computational facilities. Secondly the high sample rate requires additional memory requirements when the data are archived. Reducing the sample rate to 50 would immediately reduce the load on tape and disk memory by 50%.

3) The ANTELOPE system appears to be operating as expected, routinely detecting and locating events. However, the location errors described above are the result of using an inappropriate velocity model. The system uses the *iasp91* model (*Kennett and Engdahl*, 1991). While this model is probably adequate for locating distant (teleseismic) events in continental regions, it leads to large location errors, as much as 50-100 km, for regional events.

4) Variability of lithospheric structure is revealed by the need for different models for the regions of the northwest of Saudi Arabia (the Gulf of Aqabah/Dead Sea), the Arabian Shield and the Arabian Platform. Travel time analysis and surface wave group velocities confirm the variability in structure and the need for path-dependent models.

5) We measured surface wave group velocities for a number of earthquakes with paths sampling the Arabian Platform. Inclusion of these measurements in a tomography study shows a rich pattern of structure. This type of analysis, if continued, promises to reveal detailed structure of the seismic structure of Arabian Plate.

6) Detailed analysis of the March 11, 2002 Masafi, UAE earthquake shows that much can be learned about earthquakes and earth structure from the SANDSN waveform data, especially when combined with other data assets. The focal mechanism, depth and seismic moment of this event are well-constrained by the SANDSN data.

REFERENCES

Al-Amri, A.M. (1995 b). Preliminary seismic hazard assessment of the southern Red Sea region, *J Europ. earthq. Eng.* 3, 33-38.

Al-Amri, A. M., F. R. Schult, and C. G. Bufe (1991). Seismicity and aeromagnetic features of the Gulf of Aqabah (Elat) region, *J Geophys. Res.* 96, 20179-20185.

Al-Amri, A. M. (1998). The crustal structure of the western Arabian Platform from the spectral analysis of long-period P-wave amplitude ratios, *Tectonophysics,* 290, 271-283.

Al-Amri, A. M. (1999). The crustal and upper-mantle structure of the interior Arabian platform, *Geophys. J. Int.,* 136,421-430.

Al-Amri, A. M., R. Mellors and F. Vernon (1999). Broadband seismic noise charateristics of the Arabian Shield, *The Arabian Journal for Science and Engineering*, **24**, 2A, 99-113.

Al-Amri, M. S. and A. M. Al-Amri (1999). Configuration of the Seismographic networks in Saudi Arabia, *Seism. Res. Lett.*, 70, 322-331.

Badri, M. (1991). Crustal structure of central Saudi Arabia determined from seismic refraction profiling, *Tectonophysics,* 185, 357-374.

Ben-Menahem, A. (1979). Earthquake catalogue for the Middle East (92 BC - 1980 *AD).Boll. Geofisica Teor. Appl.* 21, 245-310.

Benoit, M., A. Nyblade, J. VanDecar and H. Gurrola (2002). Upper mantle P wave velocity structure and transition zone thickness beneath the Arabian Shield, *Geophys. Res. Lett.,* 30.

Bohannon, R. G., C. W. Naeser, D .L. Schmidt, and R.A. Zimmerman (1989). The timing of uplift, and rifting peripheral to the Red Sea: a case for passive rifting? *J. Geophys. Res., 94,* 1683-1701.

Camp, V. E., and M. J. Roobol (1992). Upwelling asthenosphere beneath western Arabia and its regional implications, *J. Geophys. Res., 97,* 15255-15271.

Christensen, N. and W. Mooney (1995). Seismic velocity structure and composition of the continental crust: A global view, *J. Geophys. Res.,* 100, 9761-9788.

Debayle, E., J. J. Lévêque, and M. Cara (2001). Seismic evidence for a deeply rooted low-velocity anomaly in the upper mantle beneath the northeastern Afro/Arabian continent, *Earth Plan. Sci. Lett., 193,* 423-436.

Gettings, M., H. Blank, W. Mooney and J. Healey (1986). Crustal structure of southwestern Saudi Arabia*, J. Geophys. Res.,* 91, 6491- 6512.

Ginzburg, A., J. Makris, K. Fuchs, C. Prodehl, W. Kaminski and U. Amitai (1979). A seismic study of the crust and upper mantle of the Jordan-Dead Sea Rift and their transition toward the Mediterranean Sea, *J. Geophys. Res*., 84, 1569-1582.

Gitterman, Y. and A. Shapira (2002). Dead Sea seismic calibration experiment contributes to CTBT monitoring, *Seismo. Res. Lett*., 72, 159-170.

Hearn, T. and J. Ni (1994). Pn velocities beneath continental collision zones: the Turkish-Iranian Plateau, *Geophys. J. Int*., **117**, 273-283.

Jackson, J., and T. Fitch (1981). Basement faulting and the focal depths of the larger earthquakes in the Zagros mountains (Iran), *Geophys. J. R. astron. Soc.,* 64, 561-586.

Kadinsky-Cade, K., M. Barazangi, J. Oliver and B. Issacks (1981). Lateral variations of high-frequency seismic wave propagation at regional distances across the Turkish and Iranian Plateaus, *J. Geophys. Res*., 86, 9377-9396.

Kennett, B. and E. R. Engdahl (1991). Travel times for global earthquake location and phase identification, *Geophys. J. Int.,* 105, 429-465.

Mechie, J., C. Prodehl and G. Koptschalitsch (1986). Ray path interpretation of the crustal structure beneath Saudi Arabia, *Tectonophysics,* 131, 333-351.

Mellors, R., F. Vernon, V. Camp, A. Al-Amri, and A. Gharib (1999).Regional waveform propagation in the Saudi Arabian Peninsula, *J. Geophys.Res., 104, no. B9,* 20221-20235.

Mokhtar, T. and M. Al-Saeed (1994). Shear wave velocity structures of the Arabian Peninsula, *Tectonophysics,* 230, 105-125.

Mooney, W., M. Gettings, H. Blank and J. Healy (1985). Saudi Arabian seismic refraction profile: a traveltime interpretation of crustal and upper mantle structure, *Tectonophysics,*111, 173-246.

Myers, S. C., W. R. Walter, K. Mayeda and L. Glenn (1999), Observations in support of Rg scattering as a source of explosion S waves: regional and local recordings of the 1997 Kazakhstan depth of burial experiment, *Bull. Seism. Soc. Am.,* 89, 544-549.

Peterson, J. (1993). Observations and modeling of seismic background noise, U.S. Geological Survey Open-File Report 93-322, Albuquerque, NM, 94 pp.

Randall, G.(1994). Efficient calculation of complete differential seismograms for laterally homogeneous earth models, *Geophys J.Int.,* 118, 245-254.

Ritsema, J., H. J. van Heijst, J. H. Woodhouse (1999). Complex shear wave velocity structure beneath Africa and Iceland, *Science, 286,* 1925-1928.

Rodgers, A., W. Walter, R. Mellors, A. M. S. Al-Amri and Y. S. Zhang (1999). Lithospheric structure of the Arabian Shield and Platform from complete regional waveform modeling and surface wave group velocities, *Geophys. J. Int*., 138, 871-878.

Rodgers, A., A. Al-Amri, A. Ar-Rajehi, T. Al-Khalifah, M. Al-Amri, M. Al-Haddad and N. Al-Arifi (2001). Analysis of regional travel time data from the November 1999 Dead Sea explosions observed in Saudi Arabia, Lawrence Livermore National Laboratory Informal Document, UCRL-ID-138770.

Rudnick, R. and D. Fountain (1995). Nature and composition of the continental crust: a lower crustal perspective, *Rev. Geophys*., 33, 267-309.

Sandvol, F., D. Seber, M. Barazangi, F. Vernon, R. Mellors and A. Al-Amri (1998). Lithospheric velocity discontinuities beneath the Arabian Shield, *Geophys. Res. Lett., 25,* 2873-2876.

Sandvol, E., D. Seber, A. Calvert and M. Barazangi (1998). Grid search modeling of receiver functions: Implications for crustal structure in the Middle East and North Africa, *J. Geophys. Res*., 103, 26,899.

Schmidt, D.L., D. G. Hadley, and D. B. Stoeser (1979). Late Proterozoic crustal history of the Arabian Shield, southern Najd province, Kingdom of Saudi Arabia, evolution and mineralization of the Arabian-Nubian Shield, *I.A.G. Bull., 3,* 41-58.

Seber, D. and B. Mitchell (1992). Attenuation of surface waves across the Arabian Peninsula, *Tectonophysics,* 204, 137-150.

Seber, D., M. Vallve, E. Sandvol, D. Steer and M. Barazangi (1997). Middle East tectonics: applications of geographical information systems (GIS), *GSA Today,* February 1997, 1-5.

Sweeney, J. (1996). Accuracy of teleseismic event locations in the Middle East and North Africa, Lawrence Livermore National Laboratory Informal Document, UCRL-ID-125868.

VanDecar, J. and R. Crosson (1990). Determination of teleseismic relative phase arrivals using multi-channel cross-correlation and least-squares, *Bull. Seism. Soc. Am*., 80, 150-169.

Vernon, F. and J. Berger (1997). Broadband seismic characterization of the Arabian Shield, Final Scientific Technical Report, Department of Energy Contract No. F 19628-95-K-0015, 36 pp.

Walter, W. (1993). Source parameters of the June 29, l992 Little Skull Mountain earthquake from complete regional waveforms at a single station, *Geophys. Res. Lett.,* 20, 403-406.

RESPONSE TO COMMENTS AND SUGGESTIONS

we are glad that the reviewers confirmed that we followed closely the original research plan and the research objectives are fully accomplished. The analysis presented shows that exhaustive analysis we were able to perform on a limited data set.

RESPONSE TO REVIEWER (2)

Comment 1. *The report lacks full detail of the software and algorithms applied to estimate event location, focal mechanism and magnitude.*

The estimation of event location, focal mechanism and magnitude is common seismological practice. The location and magnitude algorithms are embedded in the ANTELOPE software, routinely run by KACST to locate events. These methods are easily available in refereed journals and text books. Focal mechanisms are routinely estimated using the methods described in the referenced journal articles.
However, we explained in detail in the revised final report some algorithms of the ANTELOPE software which are related essentially with the scope of work.

Comment 2. *The investigators checked only the validity of their seismic velocity model for the Arabian Platform. To have higher degree of confidence in the developed seismic models and before being adopted into the SANDSN location performance operation, it is most important to test them against well-located regional events. Recent major earthquakes in Turkey or Iran are globally documented and could be used as a test case.*

Generally, the velocity models we seek must be different from the global average (iasp91). Earth structure deviates from global averages from region to region, especially in the lithosphere at the shallowest depths of the Earth (0-100 km). The greatest difference is between continental and oceanic regions. Within continental regions, significant lateral variations of seismic velocities exist between different geologic/tectonic provinces (related to thermal and chemical

heterogeneity). A global average seismic velocity model does not represent the velocity structure of specific regions within the Arabian Peninsula. The point is made clear by the mislocation errors observed in the study of the November 1999 Dead Sea explosions. Improved velocity models are needed for each region. These regions are chosen based on previous geologic studies: The Gulf of Aqabah (northwest Arabia), the Arabian Shield (Western Arabia) and the Arabian Platform (eastern Arabia). This subdivision is also justified by studies of seismic structure in the Arabian Peninsula

In our project, We had very little data to validate the arrival time picks and travel times for well-located (so called Ground Truth) events, so it was not possible to check the validity of the seismic velocity models. Ground Truth event locations are difficult to obtain. It's probably more important to locate the events within and very near the borders of the Kingdom. Events outside the Kingdom will be difficult to locate accurately without well-calibrated path-specific velocity models.

Comment 3. *In Tables 4, 5 and 6, the investigators used intentionally the word* ***"Preferred"*** *to the velocity model and also in the text. The word preferred needs clear justification. Is it a personal preference? It is indicated that the investigators selected the model that resulted in minimum residual scattering in the data. But the selection should also depend on the relevant statistical confidence level. More statistical elaboration is needed in this regard.*

It is known that the optimal model should reduce the scatter in the data (i.e. minimize the rms) and result in zero-mean residuals. We chose models that resulted in absolute mean residuals less than 0.5 seconds and minimum rms. The threshold on the absolute mean residual was chosen to be a conservative estimate on the picking error. From the 800 models considered we chose the 20 best fitting models according to the criteria described in the text. The 20 best-fitting models for both data sets are shown in Figure 19.

Consequently, The models for the 3 regions of Arabia (Gulf of Aqabah, Arabian Platform and Arabian Shield) were selected based on the fit to the available data. The Gulf of Aqabah model is based on travel times for the well-located Dead Sea explosions. The Arabian Platform and Shield models are based on the fits to complete waveforms. Again, without Ground Truth events and a large data set of travel times it is difficult to perform statistical tests of model confidence.

Comment 4 : *The research proposal stated that the expected results would lead to the development of an accurate magnitude scale for Saudi Arabia. Unfortunately, the final report does not address issue.*

Given the proposed velocity models for the 3 regions of Arabia, KACST can now re-locate the events in each region using the new models and compare the locations with independent catalog locations from well-distributed global seismic networks.

Seismic moments were determined for a few events from complete regional waveform modeling. These can be used in subsequent studies for calibrating a regional magnitude scale.

To develop a coda magnitude scale for Saudi Arabia. This will require the measurement of coda envelopes for events of various size. This provides calibration of the coda magnitude scale and seismic moments of new events can then be obtained from the measured coda envelope amplitudes. Conventional magnitude scales utilize amplitude measurements made from short time windows of narrow-band filtered direct phases such as P (Pn, Pg) or S (Sn or Lg).

Accordingly, different magnitude scales can be developed by KACST based on the aforementioned three models and availability of data in the future.

RESPONSE TO REVIEWER (3)

1. Editing mistakes, symbols and abbreviations through the entire report as well as figures (1, 2, 4, 12, 13, 15, and 32) are considered and corrected.

2. Internationally and in all scientific media, the well-known crustal structure model is written as **iasp91** NOT **IASPEI91** as shown in Bull. Seis. Soc. Am., 86, 788-796, 1996 as an example).

3. The title of the project in the English version is similar to and consistent with the Arabic version as shown below:

IMPROVING THE LEVEL OF SEISMIC HAZARD PARAMETERS IN SAUDI ARABIA USING EARTHQUAKE LOCATION AND MAGNITUDE CALIBRATION

تحسين معاملات مستوى الخطر الزلزالي في المملكه العربيه السعوديه بإستخدام موقع الزلزال ومعايرة قدره

GLOSSARY

المصطلحات اللاتينيه وترجمتها العربيه

Arabian Plate	الصفيحه العربيه
Arabian Platform	الرصيف العربي
Arabian Shield	الدرع العربي
Asthenosphere	الغلاف الوهن
Azimuth	الإتجاه الزاوي
Broadband Stations	محطات واسعة المدى
Correlation Coefficient	معامل المضاهاه
Crustal Structure	التركيب القشري
Crustal Thickness	السمك القشري
Comprehensive Test Ban Treaty Organization (CTBTO)	منظمة معاهدة حظر التجارب النوويه الشامل
Dead Sea Explosions	تفجيرات البحر الميت
Epicenter	المركز السطحي للزلزال
Focal Mechanism Solutions	حلول ميكانيكية البؤرة
Focal Depth	العمق البؤري
Ground Truth Locations	المواقع الحقيقيه الأرضيه
International Association of Seismology & Physics of the Earth (Iasp91)	نموذج حساب معدل السرعه
Frequency	التردد
Latitude (N)	خط العرض
Layer	طبقه
Lithosphere	الغلاف الصخري
Long period Spectral Ratios	نسب السعه العموديه للموجات الطوليه
Long Period Station	محطة رصد ذات فتره دوريه طويلة المدى
Longitude (E)	خط الطول
Lower Crust	القشره السفلي

Magnitude	القدر الزلزالي
Mantle	الوشاح (لحاء)
Miocene	فترة الميوسين
Moho Discontinuity	إنقطاع موهو
Monthly Listing	النشرة الزلزاليه الشهريه
Neotectonic	البنيه الحديثه
Observatory	مرصد
Origin Time	زمن حدوث الزلزال عند البؤره
Preliminary Determination of Epicenters (PDE)	التحديد المبدئي لمراكز الزلازل
Plate Tectonics	حركة الصفائح
Polar Projection	إسقاط قطبي
Primary Wave Velocity (Vp)	سرعة الموجات الطوليه
Quaternary	العصر الرابع
Receiver Function	دالة المستقبل
Response Curve	منحنى الإستجابه
Review Events Bulletin (REB)	نشرة الأحداث المراجعه
Rock Density	الكثافه الصخريه
SANDSN	الشبكه السعودية الوطنيه الرقمية للزلازل
Seismic Analysis Code (SAC)	كود التحليل الزلزالي
Seismic Attenuation	التعتيم الزلزالي
Seismic Hazards	خطر زلزالي
Seismic Noise	الضوضاء السيزميه
Seismic Tomography	زلزالية ثلاثية الأبعاد
Seismic Waves	الموجات الزلزاليه
Seismogram	سجل زلزالي
Shear Wave Velocity (Vs)	سرعة موجات القص
Spectral Amplitude	السعة الطيفيه
Spectral Analysis	التحليل الطيفي
Surface Wave dispersion	تشتت الموجة السطحي
Surficial Sediments	رواسب سطحيه
Synthetic Waveform	الشكل الموجي المركب

Take-off Angle	زاوية خروج الشعاع عند بؤرة الزلزال
Teleseismic Earthquakes	الزلازل البعيده
Tertiary	العصر الثالث
Theoretical Spectral Rations	النسب الطيفيه النظريه
Thickness	السماكه
Transfer Function	دالة المستقبل
Transition Zone	منطقة إنتقاليه
Travel Times	أزمنة المسار
Upper Crust	القشره العلويه
Wave Propagation	الإنتشار الموجي
Waveform Modeling	نمذجة الشكل الموجي